Extreme-cold-water event in the eastern Tsugaru Strait, Japan, in winter of 2014

H. Kaneko[1], Y. Miyazawa[2], H. Abe[1,3], M. Wakita[1], K. Sasaki[1], S. Watanabe[1], Y. Sato[1], T. Hashimukai[4], and S. Tatamisashi[1]

[1]Mutsu Institute for Oceanography, Japan Agency for Marine–Earth Science and Technology, 690 Kitasekine, Sekine, Mutsu, Aomori 035-0022, Japan

[2]Application Laboratory, Japan Agency for Marine–Earth Science and Technology, 3173-25 Showa-machi, Kanazawa-ku, Yokohama, Kanagawa 236-0001, Japan

[3]Graduate School/Faculty of Fisheries Sciences, Hokkaido University, 3-1-1 Minato-cho, Hakodate, Hokkaido 041-8611, Japan.

[4]Department of Marine & Earth Sciences, Marine Works Japan, 690 Kitasekine, Sekine, Mutsu, Aomori 035-0022, Japan

Corresponding author: Hitoshi Kaneko (h_kaneko@jamstec.go.jp)

Key Points:

- An extreme-cold-water event in winter 2014 in the Tsugaru Strait was investigated using observational data and a data-assimilated model
- Winter-time baroclinic instability occurred between Coastal Oyashio Water from the east and dense water inflowing from the west
- The ocean response system of the Tsugaru Strait to external disturbances, including migrating lows, was examined

Abstract (250 words)

The eastern Tsugaru Strait is an important area because it is located at the southwestern boundary of the subarctic gyre in the North Pacific, and it connects the Pacific Ocean and the Sea of Japan. Combining continuous monitoring (including fixed-point temperature measurements, shipboard observations, and high-frequency radar system observations) with a data-assimilated numerical model (JCOPE2M), we investigated the processes associated with an event characterized by extremely cold surface water observed in winter of 2014 at the southeastern side of the Tsugaru Strait. JCOPE2M outputs reproduce the event closely and reveal a low-temperature, low-salinity region of water generated from around Cape Erimo (probably by wind associated with migrating lows passing across Japan) and propagating from east to west over multiple timescales. This pattern is interpreted as representing the spreading of Coastal Oyashio Water (COW; with a density of 26.2) along the Hokkaido coast. JCOPE2M outputs also show a subsequent increase in denser water (26.6–26.8) inflowing from the Sea of Japan into the bottom of the strait. The JCOPE2M results also indicate baroclinic instability in the eastern part of the strait following the inflow of dense water. The confluence of COW and denser water is presumed to lead to

horizontal exchange, with cold COW riding up on the denser water, in turn generating the pronounced cold-surface-water event. Some past cold-water events correspond in timing to negative anomalies of the West Pacific pattern, which suggests the important influence of southward shifts in storm-track latitude of migrating atmospheric lows across Japan.

Plain Language Summary (200 words)

The eastern Tsugaru Strait is an important area because it is a water confluence region of subarctic and subtropical water masses transported by the Tsugaru Warm Current, Coastal Oyashio Current, and meso-scale eddies. In winter of 2014, on the southeastern side of the strait, an extreme-cold-water event was observed. We investigated the event using observational data (including temperature monitoring, shipboard observations, and high-frequency radar system measurements) and an ocean data-assimilated model. We found that some eastward-migrating atmospheric lows across Japan trigger the arrival of Coastal Oyashio Water to the strait, which enhances the inflow of denser water into the strait from the west side of the strait. The confluence of Coastal Oyashio Water and denser water leads to instability in the eastern part of the strait. This instability causes water-mass exchanges in the north–south direction and ultimately gave rise to the extreme-cold-water event of 2014. The present study proposes possible triggers of extreme-cold-water events in relation to the passage of migrating lows. The timing of such events corresponds closely to southward shifts in storm-track latitude. Moreover, the study describes the response system of the Tsugaru Strait to perturbations from the North Pacific (e.g., tsunami).

1 Introduction

The Tsugaru Strait is located at the same latitude as the southern boundary of the subarctic region of the North Pacific Ocean and is one of the main passes between the open ocean and the Sea of Japan (Fig. 1a). Accordingly, the eastern Tsugaru Strait is an important confluence region of the subarctic water mass transported by the Coastal Oyahio Current originating from the Sea of Okhotsk (e.g., Murakami, 1984; Nakamura et al., 2003; Sakamoto et al., 2010) and the subtropical water masses transported by the Tsugaru Warm Current (TgWC) (e.g., Rosa et al., 2007; Kuroda et al., 2012; Kaneko et al., 2021) (Fig. 1b). In addition, another subtropical water mass transported by northward-migrating meso-scale eddies from the Kuroshio Extension sometimes occurs in the outlet of the strait (e.g., Yasuda et al., 1992; Itoh and Yasuda, 2010a, b; Itoh et al., 2014; Kaneko et al., 2015). Confluence of the nutrient-rich subarctic water and warm subtropical water sustains high marine productivity in and around the strait and favors the operation of fishing and aquaculture industries. Changes in the distribution of these water masses over various timescales, induced by phenomena such as global warming, acidification, and warm- or cold-water events, have a crucial influence on marine productivity and associated human activities.

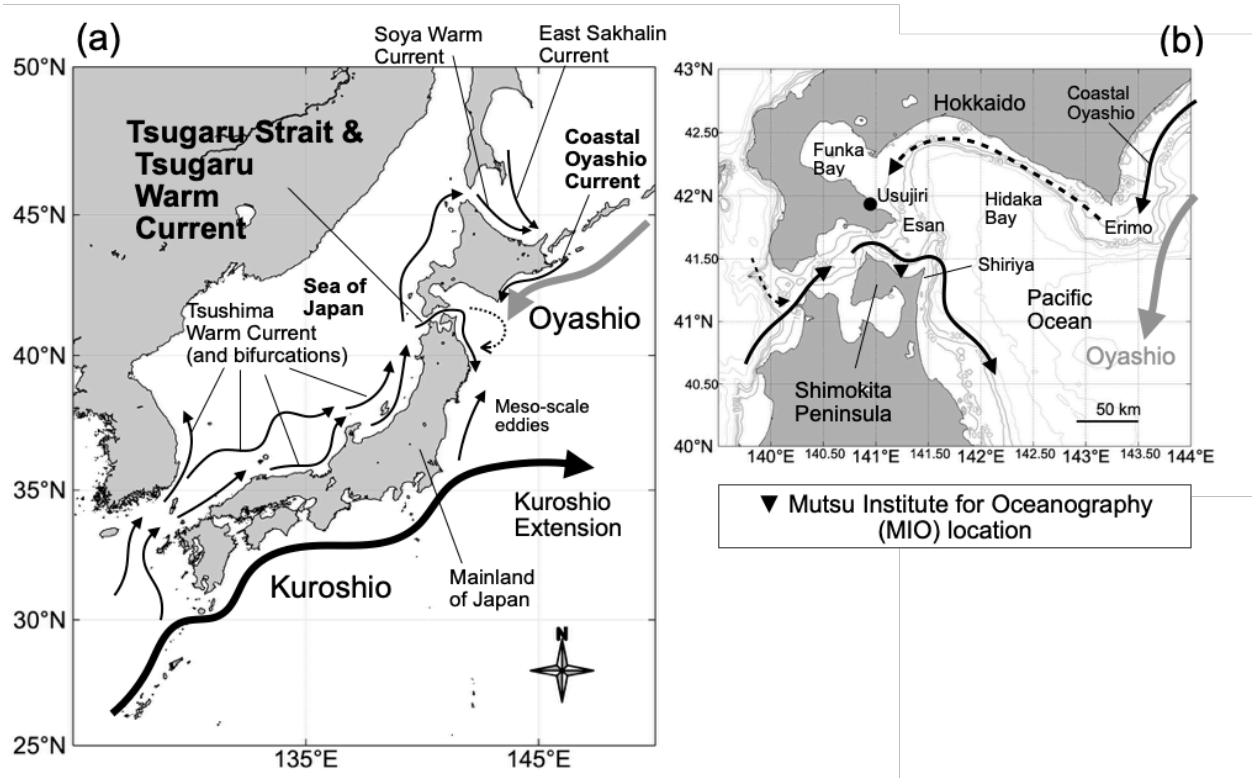

Figure 1. Schematic diagram of currents around (**a**) Japan and (**b**) the study region (the Tsugaru Strait).

Recent studies have reported more rapid acidification of the seawater in the Tsugaru Strait than in the global ocean (annual mean pH changes (decreases) at rates of -0.0051 to -0.0030 year^{-1}, Wakita et al., 2021; in the open ocean: -0.0024 to -0.0013 year^{-1}, e.g., Astor et al., 2013; Dore et al., 2009; Wakita et al., 2017). This acidification can inhibit the growth of the larvae of the Japanese scallop (*Mizuhopecten yessoensis*), which represents a major fishing industry in the vicinity of the strait. Wakita et al. (2021) also proposed that the flow of a relatively dense and deep low-pH water mass from the Sea of Japan into the strait can affect marine productivity and related industries. To track these changes in marine environments, the Mutsu Institute for Oceanography of Japan Agency for Marine-Earth Science and Technology (JAMSTEC-MIO) have expanded their monitoring system since 2002, including buoy observations, temperature monitoring, and routine seawater sampling at the institute (Wakita et al., 2021), repeated shipboard observations across the strait (Wakita et al., 2021; Kaneko et al., 2021; Yasui et al., 2022), and high-frequency radar observations of surface-water velocity (Kaneko et al., 2021; Yasui et al., 2022).

JAMSTEC-MIO temperature monitoring data recorded an extreme-cold-water event in winter (February) of 2014 (Fig. 2a–c). In that year, landing of the yellow goosefish (*Lophius litulon*) was poor, which affected fishing communities along the northern coast of the Shimokita Peninsula. Thus, investigation of the mechanisms of ocean water-mass exchange, and forecasting changes in such exchange as well as in the distribution of water masses are important both scientifically and societally in the region surrounding the Tsugaru Strait.

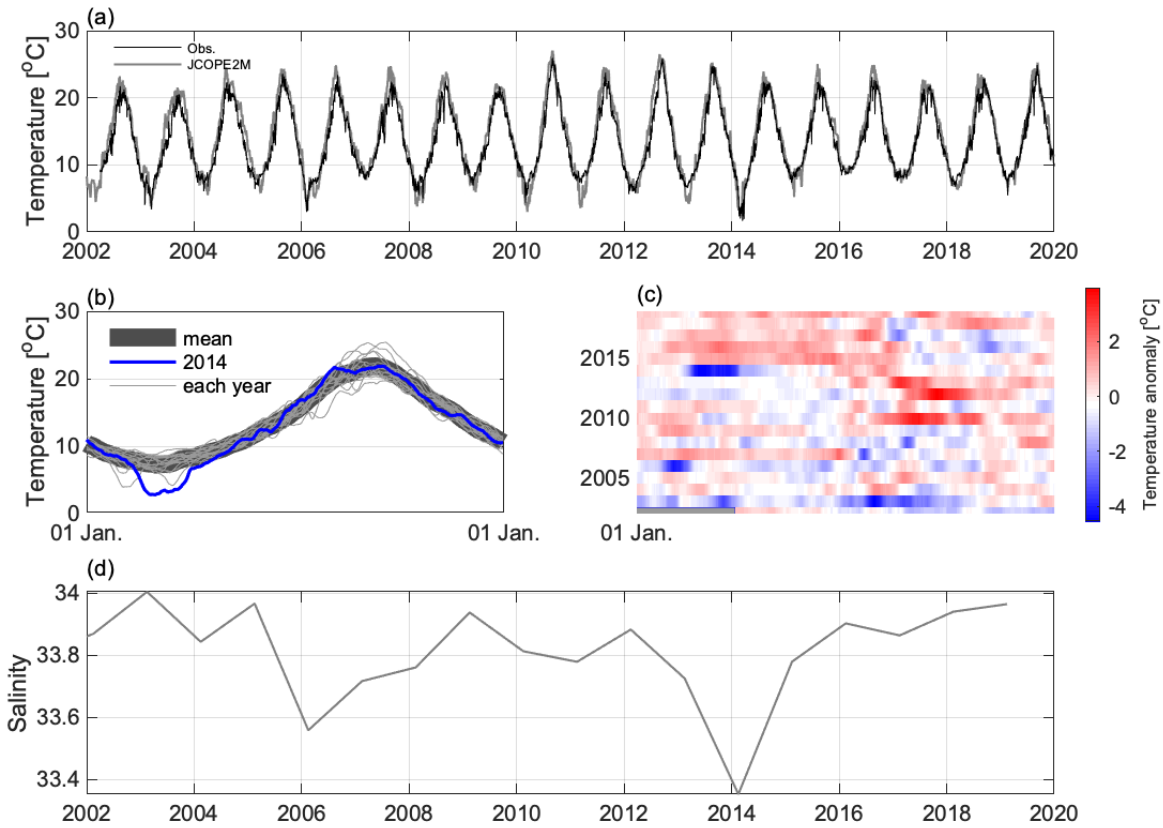

Figure 2. Time series of sea-surface temperature recorded at the Mutsu Institute of Oceanography (MIO) compared with the output of JCOPE2M. (**a**) Data for the period 2002–2019. (b) Comparison of data for different years. (**c**) Sea-surface temperature anomalies as departures from the climatological mean for the period 2002–2019. (**d**) February mean surface-water salinity estimated from JCOPE2M (41.37°N, 140.54°E, nearest grid coordinates to the MIO) for 2002–2019.

The extreme-cold-water event of 2014 was probably generated by water trans-

ported by the Coastal Oyashio Current to the east of Hokkaido Island (hereafter referred to as "Coastal Oyashio Water" or COW). However, the extension of COW to the northern coast of the Shimokita Peninsula (the southern boundary of the Tsugaru Strait; Fig 1b) is rare because warm, saline TgWC water generally flows along the coast. During winter, the density difference between the water transported by the TgWC and COW around the northern boundary of the strait is small (~0.2 kg m^{-3}; e.g., Nishida et al., 2003; Kaneko et al., 2021); therefore, the horizontal distribution of water density in the eastern part of the strait during the winter of 2014 could have been key to the occurrence of the extreme-cold-water event. Given the small density difference between COW and the water carried by the TgWC, a slight change in the density and confluence of these two water masses may lead to active water-mass exchange in the north–south direction owing to weak gravitational stability. The characteristics of the water carried by the TgWC, that is, inflow water into the Tsugaru Strait from the west, can be changed by conditions in the eastern part of the strait (Ida et al., 2016). Ida et al. (2016) used numerical modeling to hypothesize that inflow of the Japan Sea Intermediate Water (hereafter JSIW; e.g., Isobe and Isoda, 1997; Senjyu, 1999; Wagawa et al., 2020) into the strait is enhanced when the sea-level difference between the Pacific Ocean and the Sea of Japan becomes large, under the condition of a realistic narrow shelf along the western side of Hokkaido bordering the Sea of Japan (cases of sea-level difference of 1, 5, and 10 cm were used, with a width of the western shelf of 10 km). The modeling of Ida et al. (2016) was an updated version of the modeling performed by Ohshima (1994), which showed scattering of the barotropic Kelvin wave into continental shelf waves (i.e., topographic Rossby waves) having various horizontal modes (from first to third, for example; Ohshima, 1994) at the corner of the Tsugaru Strait. Ida et al. (2016) suggested that under the narrow shelf along the coast of western Hokkaido, the southward water velocity due to the lower-mode shelf wave caused by the sea-level difference exceeds the northward propagation speed of the higher-mode shelf waves along the coast (i.e., nonlinearity of barotropic continental shelf waves). Furthermore, Ida et al. (2016) suggested that the inflow of water from outside the shelf (i.e., the JSIW) increases as a result of the increase in influence of the lower mode. Arrival of cold COW at the eastern entrance of the strait itself may lead to a local negative anomaly of sea-level height and an increase in the difference in sea-surface level between the Pacific Ocean and the Sea of Japan, in turn increasing the inflow of the JSIW. Under this scenario, an increase in the inflow of the dense JSIW can also contribute to the change in density difference on the eastern side of the strait, which may cause water-mass exchange there through density flow and baroclinic instability under the weak gravitational stability.

To examine the background conditions to the extreme-cold-water event of 2014, we utilized the data-assimilated model of the Japan Coastal Ocean Predictability Experiment (multi-scale three-dimensional variational scheme) (JCOPE2M; Miyazawa et al., 2017) in addition to data obtained from temperature monitoring, shipboard observations, and high-frequency radar (HFR) (Kaneko et al.,

2021; Yasui et al., 2022). We also investigated the long-term change in the inflow water into the strait using outputs of JCOPE2M for the period 1993–2019.

The remainder of this paper is organized as follows. In Section 2, we introduce the data used in the study, including temperature monitoring data at the JAMSTEC-MIO, shipboard observations, HFR data, and numerical modeling results (i.e., JCOPE2M). In Section 3.1, we focus on the winter of 2014, comparing the observational results (temperature monitoring and shipboard observations) with results output by JCOPE2M. In Section 3.2, the low-temperature, low-salinity water regarded as COW extending alongside Hokkaido Island is investigated over multiple timescales and is compared with the speed of propagation of the shelf waves output by JCOPE2M. It should be noted that in the present study, we refer to "(continental) shelf waves" (Gill, 1982), presuming that they are Rossby waves (especially given their long wavelength) with the topographic beta effect as a restoring force, and not to "gravity waves and Kelvin waves above the continental shelf". Further, we examine the quick response of the inflow (Section 3.3) and subsequent disturbance in the eastern Tsugaru Strait (Section 3.4). Then, we discuss the characteristics of the propagating disturbance that transports COW (Section 4.1), the relationship between past cold-water events and the Western Pacific pattern index (Wallace and Gutzler, 1981) (Section 4.2), and long-term changes in the water mass within the Tsugaru Strait (Section 4.3). Finally, the results are summarized in Section 5.

2 Materials and methods

2.1 Observational data

Since 2002, the JAMSTEC-MIO, which is located on Shimokita Peninsula, southeastern Tsugaru Strait, has monitored temperature in front of the institute complex (Fig. 1b). A thermistor (R5X; Hayashi Denko, Co., Ltd) installed on a pier at the JAMSTEC-MIO has measured the sea-surface temperature (SST) every minute from 1 April 2002 to the present. Although the thermistor instrument has been changed several times, the accuracy of the sensor is a maximum of ±0.13 °C (the other cases are ±0.00 and ±0.03 °C). To detect the extreme-cold-water event of winter 2014 and to compare this event with conditions in other years, we used the time series for 2002 to 2019 using data at 10:00 (Fig. 2a–c; Japan standard time). This is because data before 2004 are recorded mostly in analog format, with only 10:00 being available in digital format for that time. In the present study, we defined "winter" as January to March.

We also used surface-current data obtained by an HFR monitoring system in the eastern Tsugaru Strait (SeaSonde, 13.9 MHz; CODAR Ocean Sensors; Kaneko et al., 2021; Yasui et al. 2022). The HFR system provides data with a horizontal resolution of ~3 km and radar coverage from ~3 to 60 km from each antenna. The distribution of surface currents is recorded every 30 minutes by the system and uploaded to the JAMSTEC-MIO Ocean Radar data Site for the eastern Tsugaru Strait (MORSETS; http://www.godac.jamstec.go.jp/morsets/e/top/).

The monitoring started in late March of 2014, just after the extreme-cold-water event. Kaneko et al. (2021) estimated the accuracy (uncertainty) of the zonal velocity of the HFR as $\pm 20 \times 10^{-2}$ m s^{-1} along a single repeated observation line between Cape Shiriya and Cape Esan (Fig. 1b). Note that in the present study, we use the HFR data simply to demonstrate the pattern of the distributions concerning the axis of the TgWC detected using the method of Kaneko et al. (2021), that is, identification of the latitude where zonal (east–west) velocity reaches a maximum for each line of longitude. Thus, the influence of the above-mentioned absolute value of the uncertainty on our conclusions is small. We used HFR data for February–March of 2014, 2017, and 2019.

In addition, three data sets obtained from shipboard observations (Table 1) were employed to compare the structures at greater depths with those estimated from the numerical model, as described below. These three data sets are (1) observations along the Hakodate–Oma line (termed the "HO-line") within the Tsugaru Strait in winter 2014 made by the training ship (T/S) *Ushio-Maru* belonging to Hokkaido University; (2) observations from stations extending southeastward from Akkeshi (southeastern coast of Hokkaido Island), termed the "A-line", collected in winter of 2014 by the research vessel (R/V) *Wakataka-Maru* belonging to the Japan Fisheries Research and Education Agency (WK1402; https://ocean.fra.go.jp/a-line/a-line_index.html); and (3) observations in the Sea of Japan conducted in autumn of 2013 by the R/V *Keifu-Maru* belonging to the Japan Meteorological Agency (KS1308; http://www.data.jma.go.jp/gmd/kaiyou/shindan/index_obs.html). Salinity, temperature, and pressure were measured by onboard conductivity–temperature–depth profilers (CTD) sensors during the cruises, using an SBE 911 plus instrument (Sea-Bird Scientific, Inc.).

Table 1. Shipboard observations made for the present study (station locations are shown in Fig. 5).

	Vessel/Ship	Region	Duration
	T/S *Ushio-Maru*	Within the Tsugaru Strait	Feb. 2014
	R/V *Wakataka-Maru*	Southeast of Hokkaido	Feb. to Mar. 2014
KS1308	R/V *Keifu-Maru*	Western Tsugaru Strait in the Sea of Japan	Oct. to Dec. 2013

Furthermore, we employed temperature measured near the sea surface (around 0.3 m, representing the minimum low tide during a year) at Usujiri (near Cape Esan; Fig. 1b) from 1989 to 2020 by the Usujiri Fisheries Station, Field Science Center for Northern Biosphere, Hokkaido University, to detect past cold-water events. We also used wind data for winter 2014 at Cape Erimo (Fig. 1b), published by the Japan Oceanographic Data Center in the online archive at https://jdoss1.jodc.go.jp/vpage/wave.html.

2.2 Ocean data-assimilated model

To investigate the background conditions of the extreme-cold-water event near the Shimokita Peninsula, we also used the outputs of the ocean data-assimilated reanalysis model JCOPE2M (the Japan Coastal Ocean Predictability Experiment, a multi-scale three-dimensional variational scheme; Miyazawa et al., 2017). JCOPE2M is based on the Princeton Ocean Model with a sigma coordinate scheme (Mellor et al. 2002), and it is driven by reanalysis data of the National Center for Environmental Prediction (NCEP) and the National Center for Atmospheric Research (NCAR) (Miyazawa et al., 2009). The range of outputs covers the western North Pacific (10.5°–62°N, 108°–180°E) with a horizontal resolution of 1/12° and 46 active vertical levels. We converted daily temperature, salinity, and horizontal water velocity from the sigma level to the following 28 depth layers: 0, −5, −10, −50, −75, −100, −150, −200, −250, −300, −400, −500, −600, −700, −800, −900, −1000, −1200, −1400, −1600, −1800, −2000, −2500, −3000, −3500, −4000, −5000, and −6000 m. Details of the configuration used have been presented by Miyazawa et al. (2017). In addition to the above-mentioned outputs, we also used daily sea-surface elevation. The period of interest for all data used in the present study is 1993–2019.

2.3 Methods

Following the method of Kaneko et al. (2021), we defined the axis of the TgWC based on the zonal velocity obtained from the HFR, as mentioned above. That is, we calculated the 24 h running mean of the zonal velocity at each grid, with the latitude of the maximum zonal velocity for each line of longitude being defined as the axis latitude. The distribution of the axis in winter and early spring of 2014, when the extreme-cold-water event occurred, was compared with that in 2017 and 2019.

The potential temperature ( ), and potential density anomaly ( ) were calculated using the profiles of temperature, salinity, and pressure following Gill (1982). Using the data obtained from JCOPE2M, we calculated the energy conversion rates from mean-to-eddy fields for kinetic energy (C'$_{\mathrm{k}}$; Eq. 1) and potential energy (C'$_{\mathrm{p}}$; Eq. 2) (e.g., Brooks and Niiler, 1977; Dewar and Baine, 1989; Kaneko et al., submitted to PEPS; hereafter K22):

$$\text{MKE to EKE: } C_k' = -\overline{u'u'}\frac{\partial \overline{u}}{\partial x} - \overline{u'v'}\left(\frac{\partial \overline{u}}{\partial x} + \frac{\partial \overline{v}}{\partial x}\right) - \overline{v'v'}\frac{\partial \overline{v}}{\partial x}, \quad (1)$$

$$\text{MPE to EPE: } C_p' = -\frac{g}{\rho_0}\overline{u'\rho'}\frac{\partial \overline{\rho}}{\partial x}\left|\frac{\partial \overline{\rho}}{\partial z}\right|^{-1} - \frac{g}{\rho_0}\overline{v'\rho'}\frac{\partial \overline{\rho}}{\partial y}\left|\frac{\partial \overline{\rho}}{\partial z}\right|^{-1}, \quad (2)$$

where u, v, and denote zonal, meridional (north–south) velocity, and density, respectively; and overbars and primes represent the temporal mean and anomalies from the temporal mean, respectively. In this study, positive values indicate energy transfer from the mean field to the eddy field. Each component of Eq. 1 is interpolated to the longitude and latitude of the temperature and salinity grid for JCOPE2M when the ratio of C'$_{\mathrm{p}}$ to C'$_{\mathrm{k}}$ is calculated.

3 Results

3.1 Extreme-cold-water event in the winter of 2014

The time series of SST at the JAMSTEC-MIO showed markedly low water temperatures (<5 °C) in the mid-winter of 2014 (Fig. 2a and b). The negative anomaly from the 2002–2019 mean for the same season was −4 °C (Fig. 2c). The extreme-cold-water event in 2014 is closely reproduced by JCOPE2M (Fig. 2a). The salinity output by JCOPE2M also shows an associated occurrence of lower-salinity water (Fig. 2d), which suggests that the low-temperature and low-salinity COW had reached the northern coast of the Shimokita Peninsula by the mid-winter of 2014, rather than the water transported by the TgWC. The studied event was important not only from the perspective of low temperature but also with regard to the dynamics of a coastal boundary current, in particular, how water in the outer zone (the northern part of the strait in this case) intrudes the inner zone (i.e., the northern coast of Shimokita Peninsula). To address this problem, we first focused on the origin of the cold water, as described below.

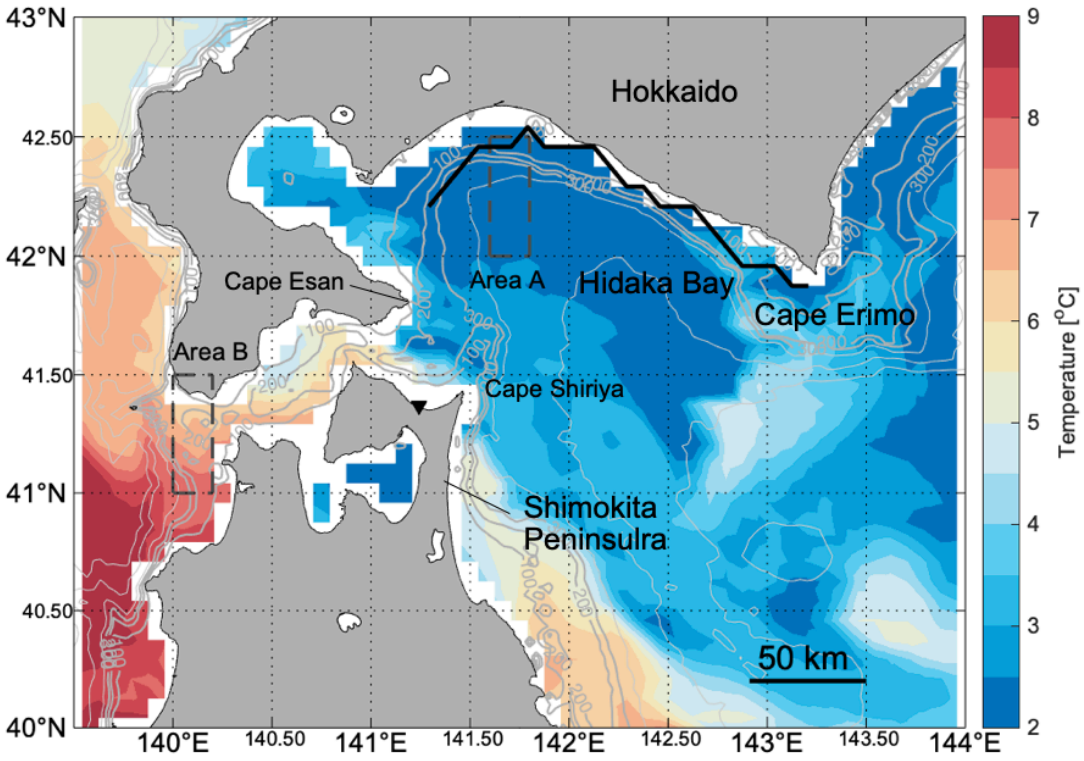

Figure 3. Distribution of sea-surface temperature generated by JCOPE2M for February 2014 (temporal mean for 18–20 February). The dashed rectangles

denote the areas used to construct the grids of potential temperature and salinity shown in Fig. 4. The black line in Hidaka Bay is the along-coast line shown in Fig. 8a. The triangle denotes the location of the Mutsu Institute for Oceanography of the Japan Agency for Marine-Earth Science and Technology.

The distribution of SST generated by JCOPE2M reveals the origin of the cold water (Fig. 3). Figure 3 shows that water with a temperature of ~2 °C is distributed in Hidaka Bay in addition to a patch in the eastern Tsugaru Strait, suggesting the influence of COW during February 2014. Using output of JCOPE2M, we compared the properties of water masses at depths shallower than 150 m in the regions to the west and east of the JAMSTEC-MIO (Fig. 4). In 2014, low-temperature and low-salinity water classified as COW ($T < 2$°C, $S < 33$; Hanawa and Mitsudera, 1987) was present in the eastern area (the rectangle located at 42.0°–42.5°N, 141.6°–141.8°E in Fig. 3; i.e., area A) according to JCOPE2M, as well as in 2010, 2011, and 2015. Moreover, water denser than Oyashio Water (> 26.6 kg m^{-3}) [and even denser than that classified as TgWC water (Hanawa and Mitsudera, 1987)] was also present in 2014. Therefore, it is inferred that in the mid-winter of 2014, the distribution of "light" (i.e., low density; <26.2 kg m^{-3}) COW in the eastern Tsugaru Strait would be dispersed around the northeastern part of the strait, which could cause the cold water to ride up onto the water transported by the TgWC near the northern coast of the Shimokita Peninsula more easily than in usual years.

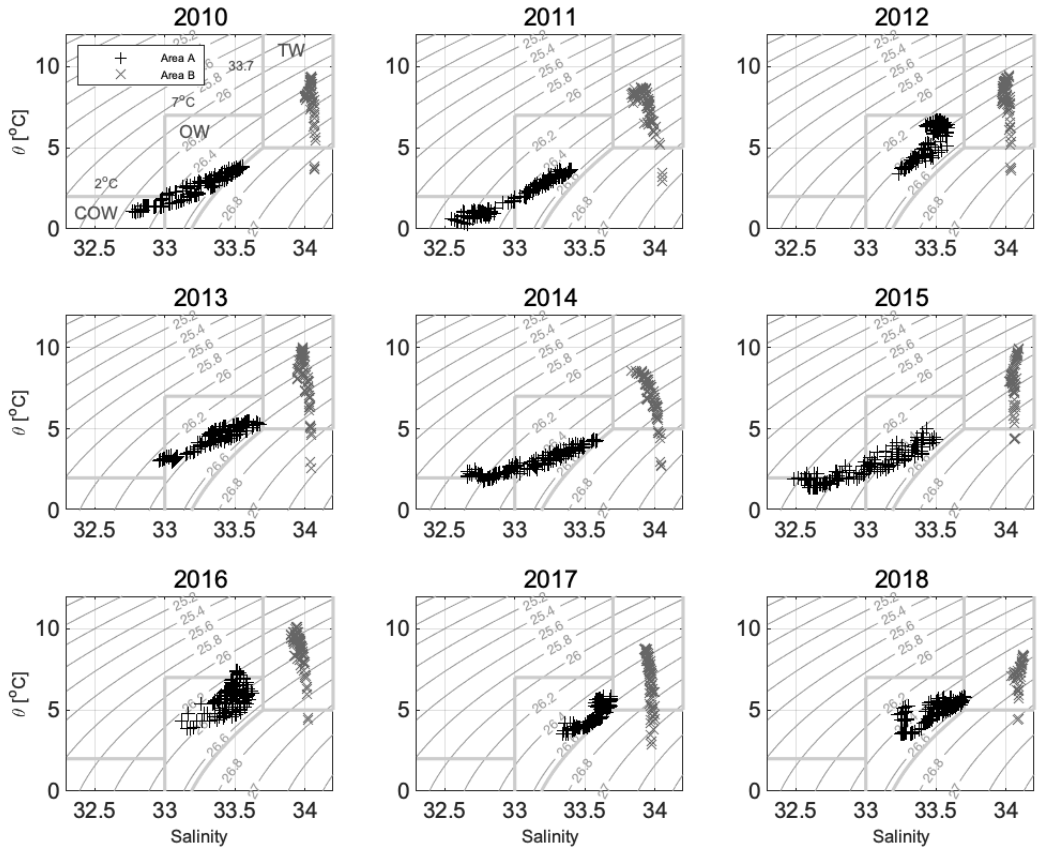

Figure 4. Potential temperature–salinity diagram for February each year for 2010–2018 (monthly isodepth mean of JCOPE2M output; 0–150 m). Light (dark) crosses denote the region of the western Tsugaru Strait (Hidaka Bay) (boxes in Fig. 3). Contours denote potential density anomaly (; kg m^{-3}). Bold light-gray lines denote the border of each water mass based on the definition proposed by Hanawa and Mitsudera (1987). COW, OW, and TW refer to Coastal Oyashio Water, Oyashio Water, and Tsugaru Warm Current Water, respectively.

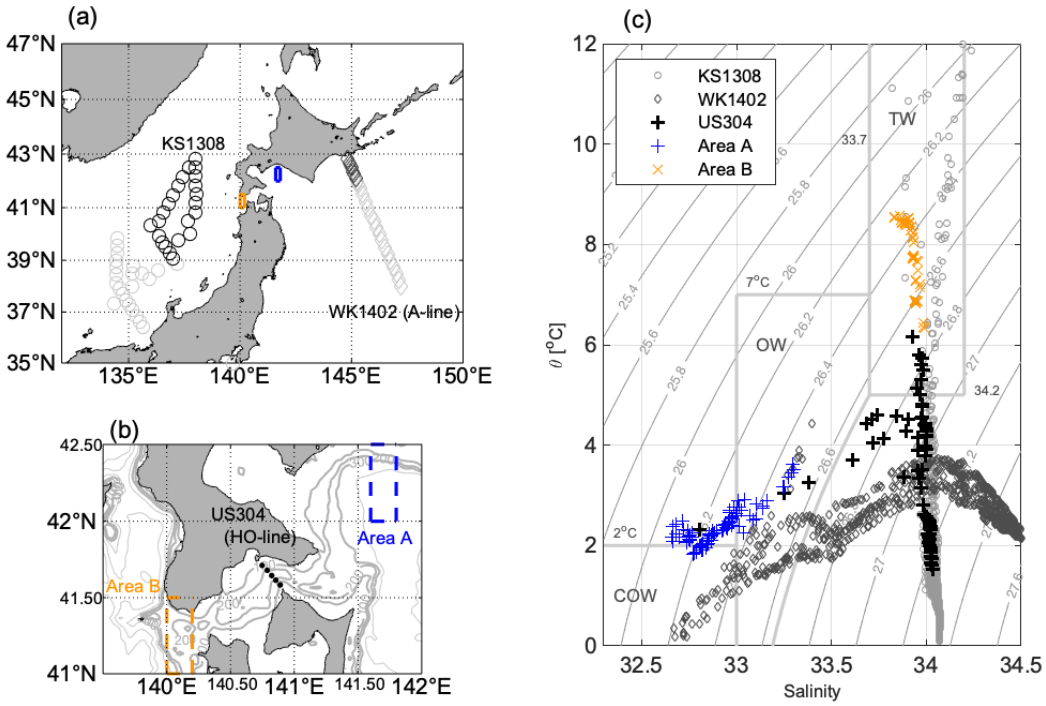

Figure 5. Patterns of potential temperature and salinity of the Sea of Japan, Tsugaru Strait, and upstream region of the Coastal Oyashio Current obtained from shipboard observations (also see Table 1). (a) Location of the shipboard-observation stations for the WK1402 and KS1308 cruises, and (b) the US304 cruise. (c) Potential temperature–salinity diagram. The monthly mean JCOPE2M outputs are superimposed as blue and orange symbols in Fig. 5c. Black circles and parallelograms in (a) are stations where the properties presented in (c) were obtained. COW, OW, and TW are same with those in Fig. 4. Contours and bold light-gray lines in (c) are the same as those in Fig. 4. The rectangles in (a) and (b) are the same as in Fig. 3. Contours in (b) indicate bathymetry (m).

Shipboard observations within the strait (HO-line) show that the water mass from greater depths of the Sea of Japan (= 1–5 °C, S = ~34, > 26.8 kg m^{-3}) entered the strait in winter of 2014 (Fig. 5). The –salinity diagrams of Fig. 5c reveal that the characteristics of the profiles along the HO-line were similar to those obtained for the Sea of Japan during the previous autumn to early winter (KS1308), suggesting that water denser than 26.6 kg m^{-3} was entering the Tsugaru Strait. According to the definition proposed by Higaki et al. (2008), water with salinity of 33.7–34.2 and density of 26.6–27.2 kg m^{-3} is classified as water of the intermediate layer of the Sea of Japan (i.e., JSIW). Thus, we refer to this dense water with high salinity (S = ~34, > 26.6 kg m^{-3}) as "JSIW" in the present study. Whereas the shipboard observations and JCOPE2M outputs

for water on the western side of the Tsugaru Strait are similar, those on the eastern side of the strait differ (Fig. 5c). A colder ($T < 2$ °C) water mass was observed in the upstream region of the Coastal Oyashio Current (WK1402) than that estimated in Hidaka Bay by JCOPE2M. This might be a result of processes such as mixing during the transport of COW from east of Hokkaido to Hidaka Bay, rather than a failure of JCOPE2M to reproduce the observations.

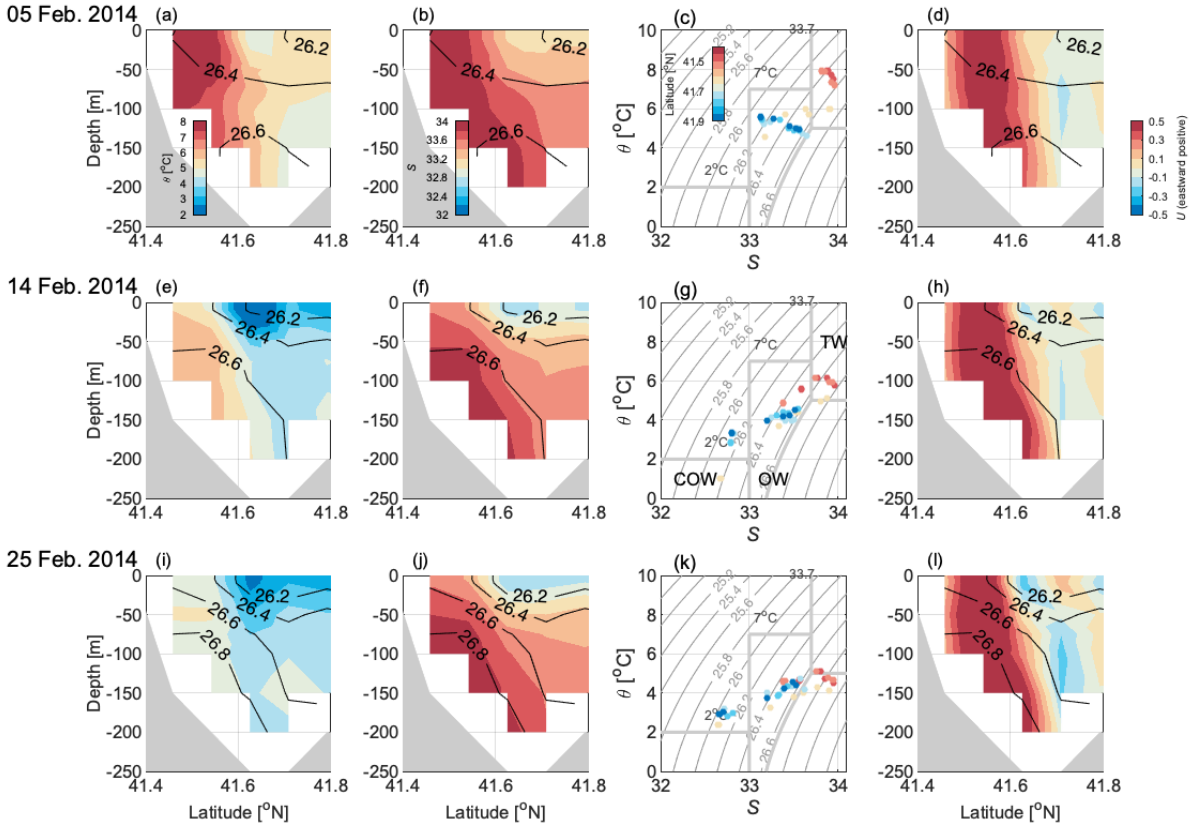

Figure 6. Diagrams of potential temperature and salinity variation with depth, –S, and zonal velocity for February of 2014 and a longitude of 141.3°E estimated by JCOPE2M. Upper, middle, and lower rows denote early, mid, and late periods in February, respectively. From the left, the columns show potential temperature ( ) sections, salinity sections, –S diagrams, and zonal velocity sections, respectively. Contours and bold light-gray lines in (c), (g), and (k) are the same as those in Fig. 4. COW, OW, and TW are the same as in Fig. 4. Black contours in the other panels represent the potential density anomaly (; kg m^{-3}).

We focus on changes in water-mass distribution in February 2014; i.e., a time scale shorter than 1 month (Fig. 6). The JCOPE2M north–south section at 141.3°E shows higher potential temperature and salinity for all plotted latitudes for early February 2014 (top row in Fig. 6) compared with later weeks, and weak stratification (Fig. 6a and b). In the and S sections and –S diagram, two types of water mass are shown (Oyashio Water distinct from COW, and TgWC water), and their density ranges are similar at ~100 m depth, with of 26.6 kg m^{-3} (Fig. 6a–c). Eastward barotropic flow near the southern boundary of the strait (i.e., near the Shimokita Peninsula) is shown and represents TgWC as a coastal boundary current (Fig. 6d). However, in mid-February (middle row of Fig. 6), potential temperature and salinity become low, and stratification is enhanced, especially at the center of the strait (Fig. 6e and f). The –S diagram for this time shows the appearance of water with very low potential temperature and salinity (Fig. 6g), suggesting the arrival of COW. Dense saline water ($>$ 26.8 kg m^{-3}, $S > 33.8$; included in the JSIW range) is identified near the bottom of the southern boundary (Fig. 6e–g). Thus, it is possible to recognize a large difference in density between COW ($<$ 26.2 kg m^{-3}) and dense water of the TgWC ($>$ 26.8 kg m^{-3}) on the southern side of the strait. That is, the horizontal distribution of density is inverted compared with the stratified season (i.e., lighter, warm, saline water on the southern side of the strait and denser, cold water on the northern side of the strait in summer; Kaneko et al., 2021; Yasui et al., 2022). Enhancement of westward flow velocity is recognized at the northern edge of the eastward-flowing TgWC (41.6°–41.7°N; Fig. 6h). After the arrival of COW, the lower potential temperature and salinity condition continues at for at least 10 days (lower row of Fig. 6), and stratification is more enhanced than that in early February between COW near the surface and the water of the bottom of the TgWC (Fig. 6i–k). The associated inclined distribution of westward water flow in the northern part of the strait is also shown (Fig. 6l), suggesting that this such baroclinic structure is maintained with a timescale of ~10 days. The presented results suggest a substantial impact of COW on the marine environment of the eastern Tsugaru Strait in February 2014.

3.2 Coastal Oyashio Water migration during the extreme-cold-water event of the winter of 2014

As rapid change (within ~10 days) in the distribution of COW in the Tsugaru Strait has been detected (Fig. 6), we focused on the origin and migration of this low-salinity water at the surface (Fig. 7). The output of JCOPE2M shows along-shore spreading of lower-salinity water from the east, around Cape Erimo to Cape Esan, and past the entrance to Funka Bay, suggesting the migration of COW in Hidaka Bay. Therefore, we constructed a distance–time map of surface salinity along the coast of Hokkaido (i.e., Hidaka Bay), westward from Cape Erimo (Fig. 8). Figure 8a shows the spread of low-salinity anomalies between January and April 2014 over two timescales: faster (~1.0 m s^{-1} or higher; arrow A in Fig. 8a) and slower [~0.1 m s^{-1}; arrow B in Fig. 8a]. There is a marked low-salinity anomaly in the distance range of −160 to −50 km with a similar slope to that of arrow A on 26 January, when the northwesterly wind (corresponding

to the monsoon in this region) at Cape Erimo changed to a northeasterly (Fig. 8b). Similar low-salinity waters appeared on various other days, including 3, 9, and 16 February. In contrast, some slower-spreading low-salinity waters (arrow B) also appeared, such as that on 26 January.

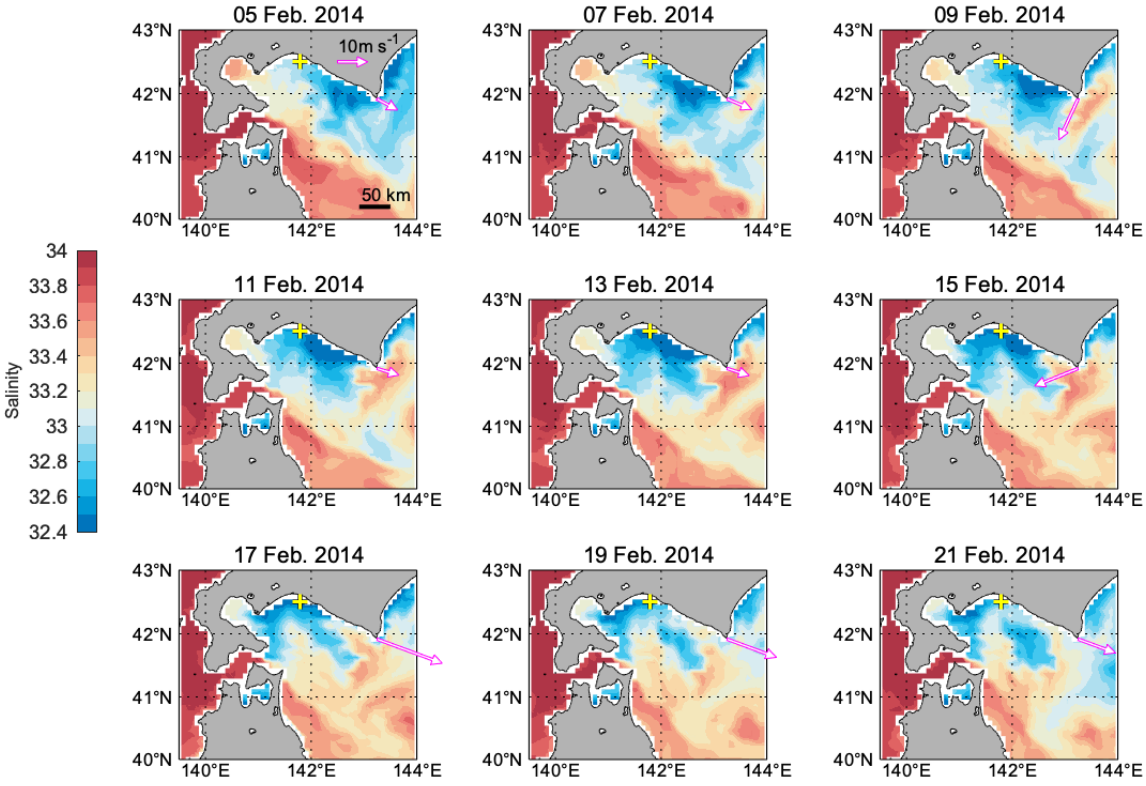

Figure 7. Distribution of surface salinity in and around the eastern Tsugaru Strait in February 2014 estimated by JCOPE2M. The magenta arrow denotes wind direction and speed at Cape Erimo. The yellow cross indicates the location of the grid of Fig. 8c.

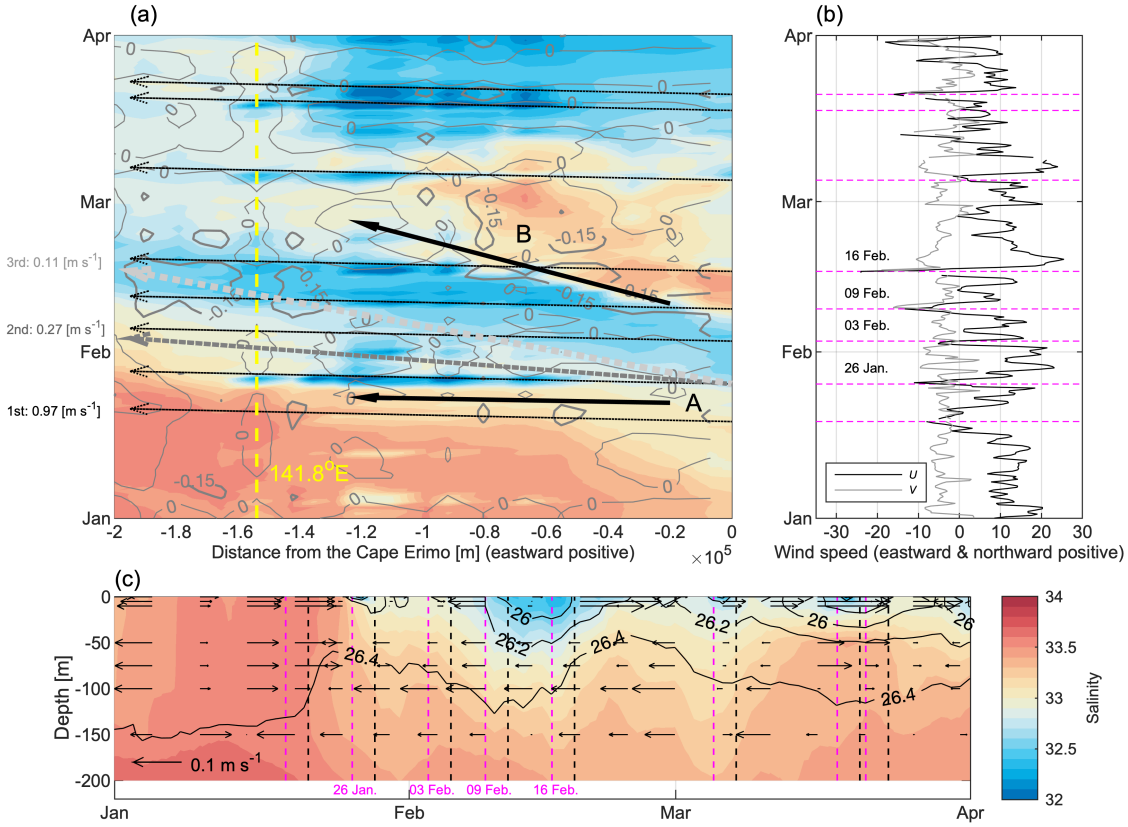

Figure 8. (**a**) Distance–time plot of surface salinity (color) and zonal sea-surface current velocity (contour; [m s^{-1}]) along the coast line (location shown in Fig. 3) of Hidaka Bay for winter of 2014 estimated by JCOPE2M. (**b**) Time series of wind speed (U is zonal, V is meridional direction; [m s^{-1}]) at Cape Esan, and (**c**) depth–time plot of salinity (color) and potential density anomaly (; [kg m^{-3}]) at 42.5°N, 141.8°E (location is shown as a yellow cross in Fig. 7). The dashed yellow line in (**a**) denotes the location (longitude) of the station in (**c**). Dashed magenta lines denote example timings of drastic changes in the zonal wind at Cape Esan (particularly when the zonal wind changes to negative). Dashed arrows in (**a**) indicate the timescale of the propagation speed of shelf waves (thin, middle, and thick denote first, second, and third modes. The solid arrows in (a) schematically represent the propagation of "fast" (arrow A) and "slow" (arrow B) salinity anomalies. The dashed black line in (**c**) indicates the timing of arrival of the first-mode shelf wave at 42.5°N, 141.8°E. Horizontal arrows in (**c**) denote zonal velocity.

In the region from Cape Erimo to Cape Esan (i.e., Hidaka Bay), propagation of velocity variations such as that of "kyucho" is known to occur (Ohshima and Miyake, 1990; Kuroda et al., 2005; Kobayashi et al., 2009). Using a barotropic model, Ohshima and Miyake (1990) suggested that the shelf waves generated by southeasterly wind on the eastern part of Hidaka Bay will propagate to the west. Kuroda et al. (2005) calculated the propagation speed of the first, second, and third modes of shelf waves at Hidaka Bay (Line 1 in their study) as 0.97 m s^{-1}, 0.27 m s^{-1}, and 0.11 m s^{-1}, respectively. Because the speeds of waves estimated by Kuroda et al. (2005) represent the characteristics and inherent magnitude of the propagation speed for shelf waves having a long wavelength (i.e., small wave number and non-dispersive) at Hidaka Bay given the bathymetry, we also employed these values. The timescale is indicated as the slope magnitude of each inclined dashed arrow in Fig. 8a.

The pattern of the low-salinity anomalies indicates a rapid response time to changes in wind (arrow A in Fig. 8a), especially changes in zonal wind direction as mentioned above, and have a similar timescale to that of first-mode shelf waves, far faster than surface-water velocity (e.g., 9 and 16 February; Fig. 8a and b; also see Text S1 and Figs S1–3 for the barotropic characteristics). It should be noted that, based on the theory of wind-forced coastal shelf waves proposed by Gill and Schumann (1974), Kuroda et al. (2005) further suggested that the propagation speed of the first mode could be faster (2.0–4.0 m s^{-1}) than that of the no-wind-forced case (i.e., ~0.97 m s^{-1}).

In contrast, the slope of the other salinity anomaly (arrow B in Fig. 8a) is similar to that of the second and third modes of the shelf waves (it should be noted here that the propagation speed is not necessarily consistent with the velocity associated with shelf waves). Kuroda et al. (2005) demonstrated that the contributions of the first mode to velocity are substantial (second: ~45% of the first mode; third: ~20% of the first mode). Thus, the correspondence of the migration timescale between salinity anomalies (arrow B in Fig. 8a) and the higher-mode propagation speed (e.g., 0.27 and 0.11 m s^{-1}), as mentioned above, may imply that after the passage of the tip of the higher-mode shelf waves, the effect of the advection of the background gradient of salinity will increase owing to the increase in along-coast current speed.

Furthermore, although the propagation speed of low-salinity water at the surface seems similar to the higher mode (Fig. 8a), the propagation exhibits a stratified structure; i.e., "light" water with low salinity near the surface is present (Fig. 8c). Therefore, these propagating disturbances are likely to have not only barotropic but also baroclinic characteristics. This complexity has been suggested by Kobayashi et al. (2009), who reported a "kyucho" event around the regions in May 2006. The characteristics of the disturbances in relation to the barotropic/baroclinic character are described in Section 4 below.

3.3 Change in sea level around Cape Esan and the immediate response of the water inflowing to the strait to the arrival of Coastal Oyashio Water

In Subsection 3.2, two types of salinity-anomaly migration in Hidaka Bay were suggested: faster and slower. Thus, considering those timescales, we examined the effect of the arrival of COW into the region of Cape Erimo (Fig. 9a) on sea-level change. The results show that after pronounced changes in wind speed and direction at Cape Erimo, as shown in Fig. 9b for the component of the southeast–northwest direction (26 January and 9 February; southeastward positive), the salinity of water at 5 m depth near Cape Esan estimated by JCOPE2M ($\langle S_{5\mathrm{m}} \rangle$) decreases rapidly (from ~33.5 to ~33.2 and from 33.1 to 32.6, respectively; Fig. 9c). Then, considering the sea-surface level between the Pacific side and the Sea of Japan side, the sea-surface level estimated from JCOPE2M outputs shows that as a general condition, the level on the Sea of Japan side is higher than that at Cape Erimo ($\langle \mathrm{SSH} \rangle_{\mathrm{Esan}}$) (Fig. 9b). In addition to this background difference in the sea-surface level, the difference (Sea of Japan minus Cape Erimo; $\langle \mathrm{SSH} \rangle$) tends to increase after the pronounced change in along-coast wind speed at Cape Erimo (26 January and 3, 9, and 16 February; Fig. 9b) with a lag of several days (Fig. 9c). The wavelet transform between $\langle \mathrm{SSH} \rangle$ and $\langle S_{5\mathrm{m}} \rangle$ for 2014 suggests a close relationship between these variables for a period of 5–8 days, from late January to early February (Fig. 9d); i.e., the lower-salinity anomaly near Cape Erimo corresponds to a large sea-level difference between the Sea of Japan and the area near Cape Erimo from late January to early February. Note that this timescale (5–8 days) is consistent with that for significant variation in both along-shore current speed and wind stress at Hidaka Bay (6.5 days) reported by Kuroda et al. (2005).

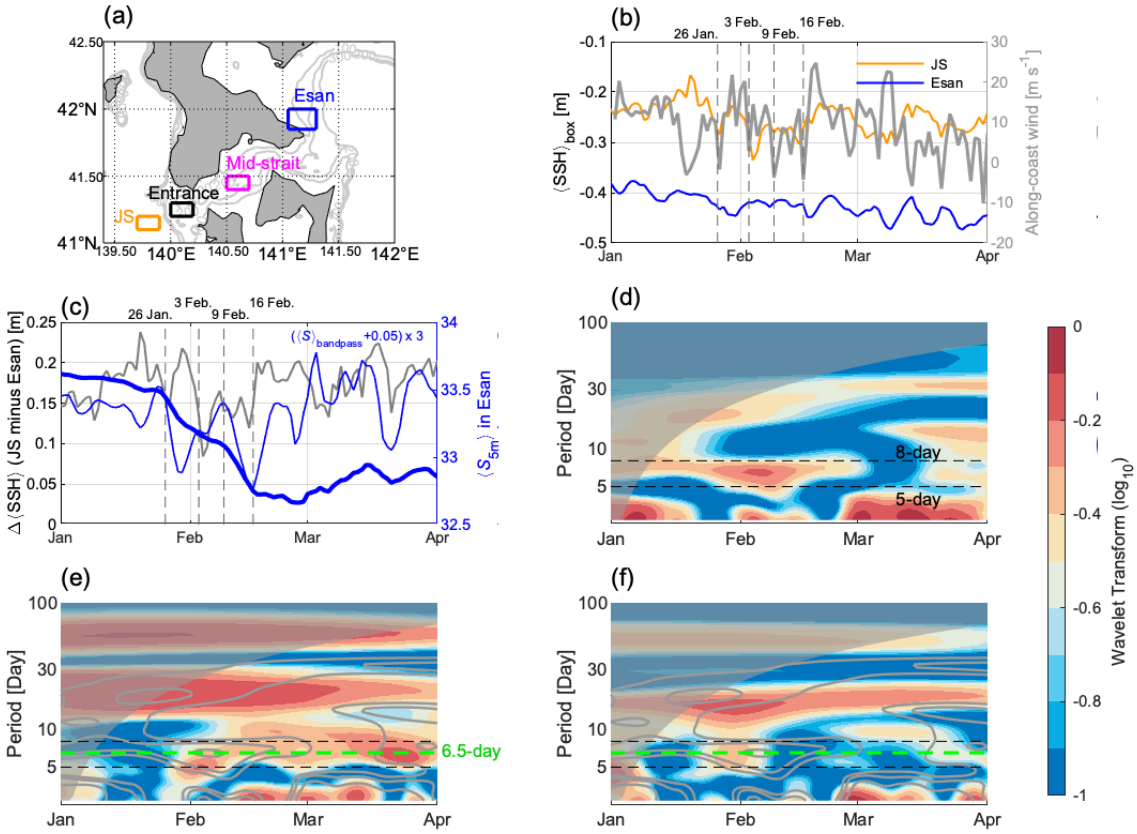

Figure 9. (a) Locations of analyzed sub-regions (JS denotes the Sea of Japan). Time series of (b) sub-region-averaged sea-surface level in the JS and Esan sub-regions ($\langle \mathrm{SSH} \rangle_{\mathrm{JS}}$ and $\langle \mathrm{SSH} \rangle_{\mathrm{Esan}}$, respectively) and along-coast wind at Cape Erimo from January to March 2014 estimated using JCOPE2M, and (c) difference in the elevation ($\langle \mathrm{SSH} \rangle$) of the JS sub-region with respect to the Esan sub-region ($\langle \mathrm{SSH} \rangle_{\mathrm{JS}} - \langle \mathrm{SSH} \rangle_{\mathrm{Esan}}$) compared with sea-water salinity at 5 m in the Esan sub-region. Thick and thin blue lines in (c) are sub-region-averaged salinity ($\langle S_{5\mathrm{m}} \rangle$) and band-passed salinity ($\langle S_{\mathrm{bandpass}} \rangle$; 5–8 days), respectively. Wavelet transform between (d) $\langle \mathrm{SSH} \rangle$ and $\langle S_{5\mathrm{m}} \rangle$, (e) $\langle \mathrm{SSH} \rangle_{\mathrm{Esan}}$ and 4-day-delayed along-coast wind, and (f) $\langle \mathrm{SSH} \rangle_{\mathrm{Esan}}$ and 15-day-delayed along-coast wind.

We also examined the time-lagged relationships between $\langle \mathrm{SSH} \rangle_{\mathrm{Esan}}$ and along-coast wind at Cape Erimo. The results show that 4- and 15-day-delayed wavelet transforms show maxima in a 5–8-day period in early February (Fig. 9e and f). This suggests that faster and slower migrations of the salinity anomaly from

Cape Erimo to Cape Esan would affect sea-surface level as well as salinity in the region around Cape Esan, and also the sea-surface level difference between the Pacific and the Sea of Japan (note that the advection speed is not necessarily similar to the phase speed, which would lead to the lags). The numerical experiment of Ida et al. (2016) demonstrated that an increase in the difference in sea level between the Pacific Ocean and the Sea of Japan could cause an increase in inflow of the denser JSIW into the Tsugaru Strait under realistic bathymetric conditions. Therefore, the arrival of COW in 2014 estimated by JCOPE2M outputs could also lead to such a response to the inflow. Thus, we focused on the salinity of near-bottom water in the western entrance and central part of the Tsugaru Strait (black and magenta boxes in Fig. 9a, respectively).

From mid-January to mid-February, the salinity of water at a depth of 150 m in the entrance region and $\langle \mathrm{SSH} \rangle$ show a close relationship, with an inverse relationship over a timeframe of several days, and a greater sea-level difference being associated with a low near-bottom salinity (Fig. 10a). During mid-January to mid-February, the lower salinity suggests denser water; i.e., the JSIW (Fig. 10b). In contrast, from mid-February to mid-March, the large $\langle \mathrm{SSH} \rangle$ tends to correspond to higher salinity in near-bottom water, with the higher salinity suggesting denser water (Fig. 10b). In any case, large $\langle \mathrm{SSH} \rangle$ during mid-winter would suggest the entry of dense water into the near-bottom region of the entrance to the strait. The temporal variation in salinity within the central part of the strait is generally similar to that in the entrance region, especially during early to mid-February (Fig. 10c).

A depth–time section of salinity and density within the strait estimated by JCOPE2M outputs shows a marked response of JSIW inflow from the Sea of Japan to drastic wind change at Cape Erimo with a 4 day lag; i.e., the JSIW inflow occurs immediately after the arrival of the low-salinity anomaly (e.g., 30 January and 7, 13, and 20 February; Fig. 10d). It is thought that the external Kelvin wave probably exits the strait immediately (Gill, 1976) and affects the inflow water into the strait (Ohshima, 1994; Ida et al., 2016).

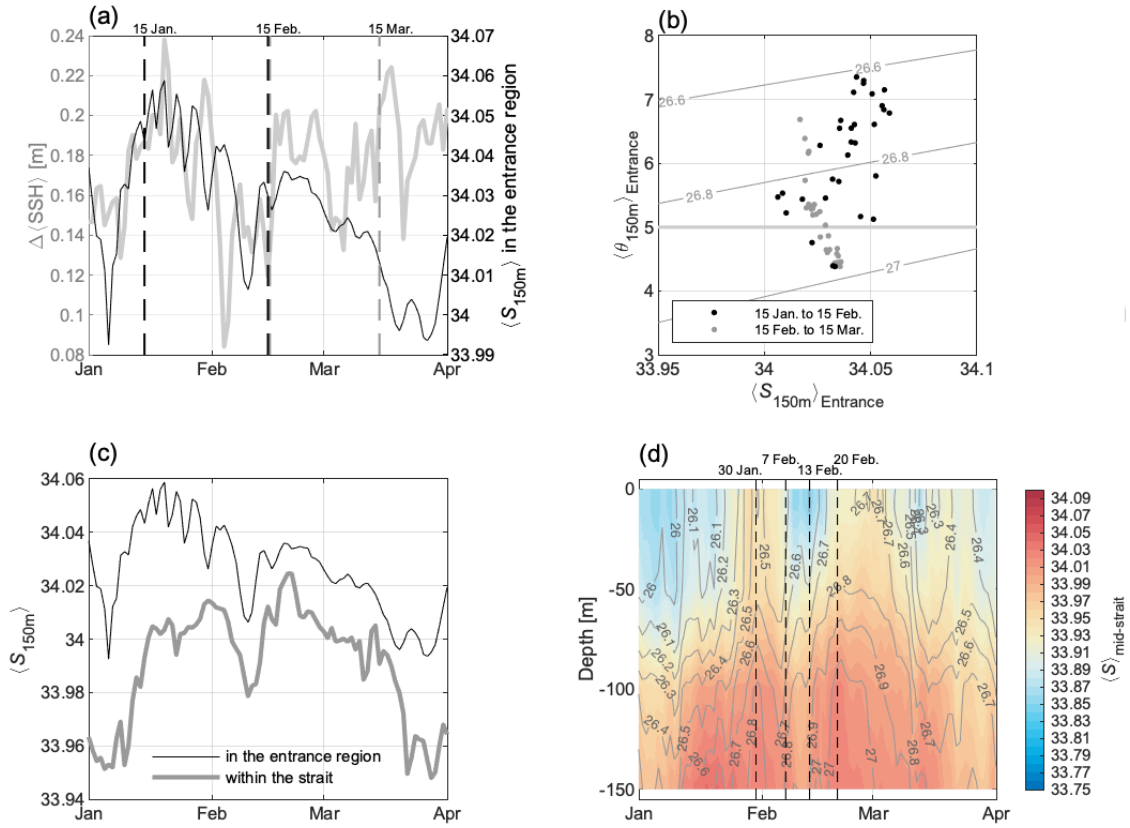

Figure 10. (a) Time series of sea-surface level difference between the Sea of Japan and the Cape Esan region (orange and blue boxes in Fig. 9a, respectively; i.e., ⟨SSH⟩). (b) Area-averaged potential temperature plotted against that of salinity at 150 m depth for the period 15 January to 15 March 2014 in the entrance region of the Tsugaru Strait (black box in Fig. 9a). (c) Time series of salinity at 150 m depth in the entrance region and that within the strait. (d) Depth–time plot of salinity (color) and potential density anomaly (contour; kg m^{-3}) within the strait. All results are estimated from JCOPE2M. Contours and the thick gray line (5 °C) in (b) are the same as in Fig. 4.

3.4 Baroclinic instability in the eastern Tsugaru Strait after inflow of Japan Sea Intermediate Water

Although it is expected that the arrival of light COW at the northeastern part of the Tsugaru Strait and subsequent flow of denser water from the opposite side of the strait to the eastern part of the strait eventually contributed to stratification via some disturbance, such as density flow, the exact process remains unclear.

HFR results suggest large variation in the latitude of the TgWC axis in the eastern part of the strait from mid-March to early April of 2014, and thus a frontal disturbance such as baroclinic instability for several weeks (Figs 11 and S4); that is, slower processes with a timescale of f^{-1} (where f is the local inertial frequency), which would have contributed to the February 2014 extreme-cold-water event. Using a downscaled version of an ocean data-assimilated model (JCOPE-T DA; Miyazawa et al., 2021), Kaneko et al. (K22) demonstrated that baroclinic instability occurs in the eastern part of the strait during the stratified-water season. As a topic to address in future research, K22 also proposed that baroclinic instability may also occur in winter; i.e., the weakly stratified season in the strait (e.g., Nishida et al., 2003; Kaneko et al., 2021). As COW transported to the Tsugaru Strait has a density of $<$26.6 kg m^{-3} (i.e., lighter than the JSIW; Fig. 4), baroclinic instability is likely to be enhanced in the strait by COW. Figure 6 shows that the enhanced vertical shear of the zonal current component (u) at 41.6°N, 141.3°E in mid- and late-February 2014 occurred under conditions favoring baroclinic instability. Therefore, we calculated the energy conversion rate from mean potential energy to eddy potential energy using JCOPE2M outputs (Fig. 12).

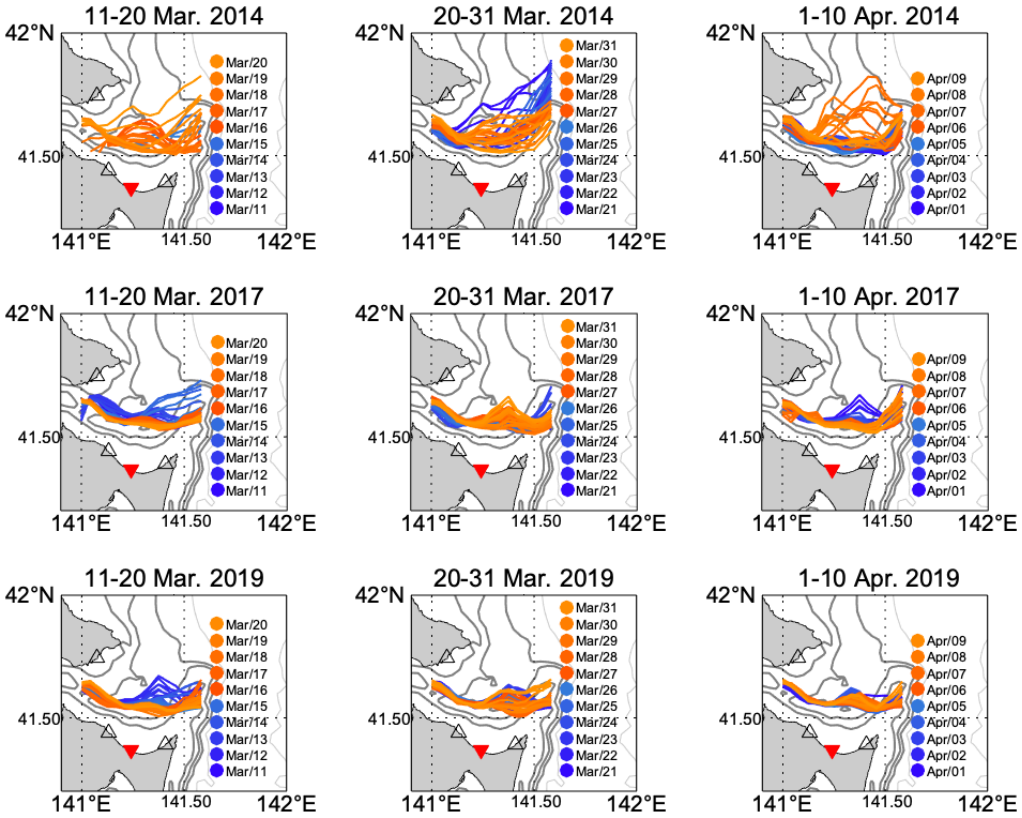

Figure 11. Location of the axis of the Tsugaru Warm Current estimated from the HFR system during late March of 2014, 2017, and 2019. Black-outlined triangles denote the locations of the radar antenna. The red triangle denotes the location of the Mutsu Institute for Oceanography of Japan Agency for Marine-Earth Science and Technology. Note that because of a lack of observations for February 2014, we show here the situations for late March. The equivalent diagrams for February 2017 and 2019 are presented in Figure S4.

The estimated energy conversion rate of potential energy (C'_{p}) at the surface during 11–20 February 2014 shows a high positive value [$\sim O(10^{-6})$ m^2 s^{-3}] in the center of the eastern part of the strait (Fig. 12a). This value is larger than that estimated for Kuroshio by Itoh and Sugimoto (2008) based on moorings at depths of 250–1250 dbar during April 2003 to March 2004 [$O(10^{-7})$ m^2 s^{-3}] (note that at depths greater than 20 m, the magnitude estimated in the present study is similar to that of Ioth and Sugimoto, 2008). The ratio of C'_{p} to C'_{k} in the center of the eastern part of the strait is high, suggesting dominance of the

energy conversion of potential energy over that of kinetic energy in that area; i.e., there was significant baroclinic instability near the surface in the eastern part of the strait during February 2014.

A depth–time plot of C'_{p} at 41.5°N, 141.3°E shows positive values from early-February and near-surface maxima during mid-February (Fig. 12c). During mid- to late-February, stratification intensifies, and low-salinity water appears near the surface (Fig. 12c), suggesting that baroclinic instability caused north–south water-mass exchange and subsequent stratification in the eastern part of the strait for the longer timescale of f^{-1}. This result is consistent with those obtained from HFR and can explain the 2014 extreme-cold-water event near the Shimokita Peninsula.

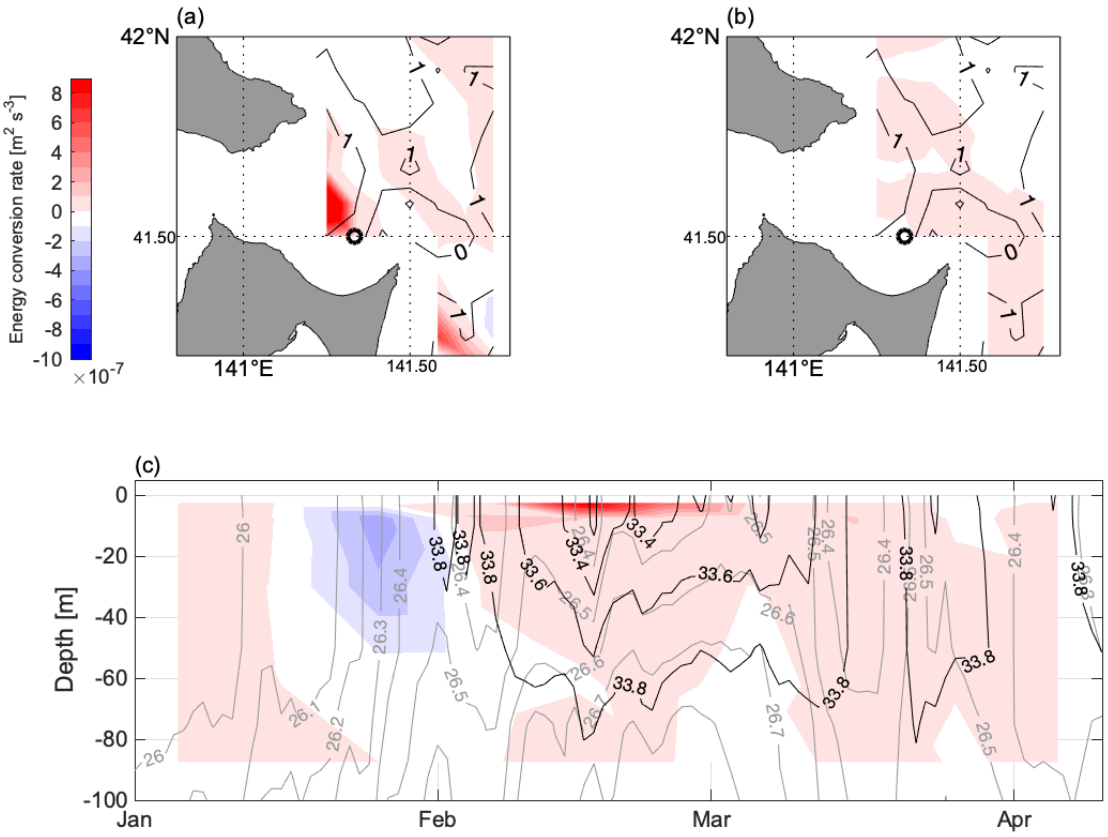

Figure 12. Energy conversion rate of (**a**) potential energy (C'_{p}) and (**b**) kinetic energy (C'_{k}) during 11–20 February 2014 estimated from JCOPE2M (positive: mean-to-eddy conversion). Contours in (**a**) and (**b**) denote the ratio of the absolute value of the baroclinic energy conversion rate to that of

barotropic energy conversion in logarithmic scale. (**c**) Depth–time section of C'_{p} at 41.5°N, 141.3°E (circle in **a** and **b**). Black (gray) contours in (**c**) denote salinity (potential density anomaly; [kg m^{-3}]).

4 Discussion

4.1 Characteristics of the migration of the low-salinity anomaly generated at Cape Erimo

In the present study, the results of JCOPE2M suggest that local atmospheric variation (when the northwesterly monsoon around Cape Erimo weakened and the wind direction underwent a pronounced change) associated with migrating lows in mid-latitude regions could have generated westward-propagating perturbations along Hidaka Bay during winter 2014 (Fig. 8a and b). On 9 and 16 February, for example, when sharp and pronounced changes in wind direction were observed (Fig. 8b), developing lows passed south of Erimo and brought the heaviest snowfall in recorded history to some areas around Tokyo (Fig. S5). A similar situation with an abrupt change in wind direction occurred on 26 January and in mid-March (Fig. 8b). The wind variation associated with the migrating low, such as the northeasterly wind on 9 February in the vicinity of Cape Erimo (Figs 7 and 8b), might have caused southward migration of COW across the submarine topography at the cape owing to wind stress near the sea surface, although Kono et al. (2004) suggested that entry of the baroclinic Coastal Oyashio Current into Hidaka Bay can be inhibited by the joint effect of baroclinicity and bottom relief (JEBAR) (Shaw and Csanady, 1983; Huthnance, 1984; Csanady, 1985; Mertz and Wright, 1992; Isobe, 1994). Moreover, water riding over this terrain would be moved northwestward by surface Ekman transport because of the northeasterly wind (Fig. 7). Wind direction changed from northeasterly to northwesterly on 10 February due to the passage of the migrating low south of Cape Erimo (Fig. S5), and this might have led to the temporary convergence of the low-salinity COW in Hidaka Bay near Cape Erimo horizontally due to wind stress. Furthermore, re-weakening of the northwesterly wind on 16 February (Fig. 8b) might have triggered the propagation of shelf waves and baroclinic disturbance (Fig. 8). Ohshima and Miyake (1990) demonstrated on the basis of a numerical model that propagation of the higher mode of the barotropic shelf wave is inhibited during pronounced northwesterly winds. Thus, periodic relaxation of the northwesterly monsoon might cause westward propagation of shelf waves of even higher mode. Considering the temporal variation in such local atmospheric forcing, it is likely that the "slow" salinity anomaly migration associated with the preceding migrating low (e.g., that of 26 January) was superimposed by the transfer of the "fast" salinity anomaly migration associated with the later migrating low (such as in mid-February), which could have caused large changes in sea-surface level near Cape Esan (Fig. 9).

Although stratification would probably be far weaker in winter than in summer, the vertical structure of horizontal velocity in Hidaka Bay suggests a degree of baroclinicity (Fig. 8c). It is also considered that the salinity anomaly may have

been advected by baroclinicity, including the effect of the geostrophic current near the surface (Fig. 8a), in addition to barotropic shelf waves (Text S1 and Figs S1–3). On a related note, the effect of internal Kelvin waves with the vertical first mode may also be possible instead of the higher-mode shelf waves in Fig 8a. Taking the representative density difference between the upper and lower layers of the vertical first mode ( ) as ~0.4 kg m^{-3} (Fig. 8c) and the thickness of the upper and lower layers as $H_1 = 50$ m and $H_2 = 150$ m, respectively, the phase speed of the Kelvin wave is estimated as ~0.38 m s^{-1} $\{[g \ / \ _0 \ H_1 \ H_2/(H_1 + H_2)]^{1/2}$; where g is the gravitational acceleration, and $_0$ is the reference density set as 1026 kg m$^{-3}\}$, which is comparable to the speed of the horizontal second mode of the shelf waves and spreading of the low-salinity-water region at the surface (Fig. 8a, arrow B); note that phase speed does not necessarily mean advection speed, and may be a (non-dispersive) long Kelvin wave. Murakami (1984) also estimated the speed of tips of the COW inflow for some cases from 0.12 to 1.27 m s^{-1}, using of ~0.8 kg m^{-3} and equations proposed in previous studies (e.g., Yamagata, 1980; Kubokawa and Hanawa, 1984). Thus, rapid variation in the salinity anomaly (Fig. 8a, arrow A) may also occur and affect the distribution of near-surface salinity of waters along the coast of Hidaka Bay depending on the stratification condition (Figs S1 and S2).

Although Ohshima and Miyake (1990) demonstrated that barotropic shelf waves skip Funka Bay along bathymetric contours, "lighter" COW near the surface reaching Cape Esan while skipping the bay was also estimated by JCOPE2M outputs in the present study (Fig. 6). Although the skipping of the baroclinic current around the bay may be related to the horizontal resolution of JCOPE2M (1/12°), it is expected that several processes are responsible for this phenomenon, such as overlapping of the first barotropic shelf wave skipping the bay on the prevailing baroclinic coastal boundary current flowing along Funka Bay. Further, baroclinic processes, such as JEBAR may themselves be responsible for shelf waves skipping the bay, as JCOPE2M outputs also show that enhancement of the southward-flowing surface current between 141.2° and 141.6°E at 42.1°N (near the mouth of Funka Bay within Hidaka Bay, i.e., near Usujiri; Fig. 1b) occurred in association with low temperature and salinity on 17 February 2014 (Fig. 13). Furthermore, scattering of the internal Kelvin waves at the characteristic topography (eastern part of the mouth of Funka Bay) and subsequent supply of vorticity may also be important for the formation of such offshore paths, as suggested by Igeta et al. (2017). The effects of vorticity supply at and around Funka Bay on baroclinic flow are not yet fully understood and require investigation in future studies.

As another characteristic of the baroclinic structure, we also find that relatively high-temperature patches (4–5 °C) crossing the southward-flowing current during late February of 2014 appear at densities of = 26.4–26.8 kg m^{-3} at the 42.1°N line in Hidaka Bay (the lower row of Fig. 13). Because the energy conversion rate of potential energy involves mean-to-eddy conversion (positive value of ~1 × 10^{-7} m^2 s^{-3}) in the density range at 141.7°–142.0°E for mid-February, there is a possibility of baroclinic instability and dynamic

water-mass exchanges at depths of 100–200 m between 141.5° and 142.0°E, that is, near the mouth of Funka Bay at that time. Because the density range (= 26.4–26.8 kg m^{-3}) reaches that of North Pacific Intermediate Water (e.g., Yasuda et al., 1996)—i.e., water of slightly higher density than the winter density at the sea surface of the western North Pacific—qualitative and quantitative studies of the process of discharge of water accumulated in Funka Bay into the Pacific, and the impact of this process on downstream areas, may lead to new insights into the subduction process in the western North Pacific. In addition, as baroclinic instability can contribute to subsequent stratification (e.g., Fig. 12c), such stratification from late winter to early spring may lead to favorable sunlight conditions for photosynthesis within water column, thus supporting the high biological production in the region from Funka Bay to offshore Hidaka Bay during early spring (e.g., Tanaka, 1984). Such conditions may be important for the growth of larvae of the walleye pollock (*Theragra chalcogramma*), which is one of the most important commercial fish species in Japan and spawns in winter around Hidaka and Funka bays. Therefore, additional investigation into baroclinic instability during winter in the vicinity of these bays should be conducted in future studies.

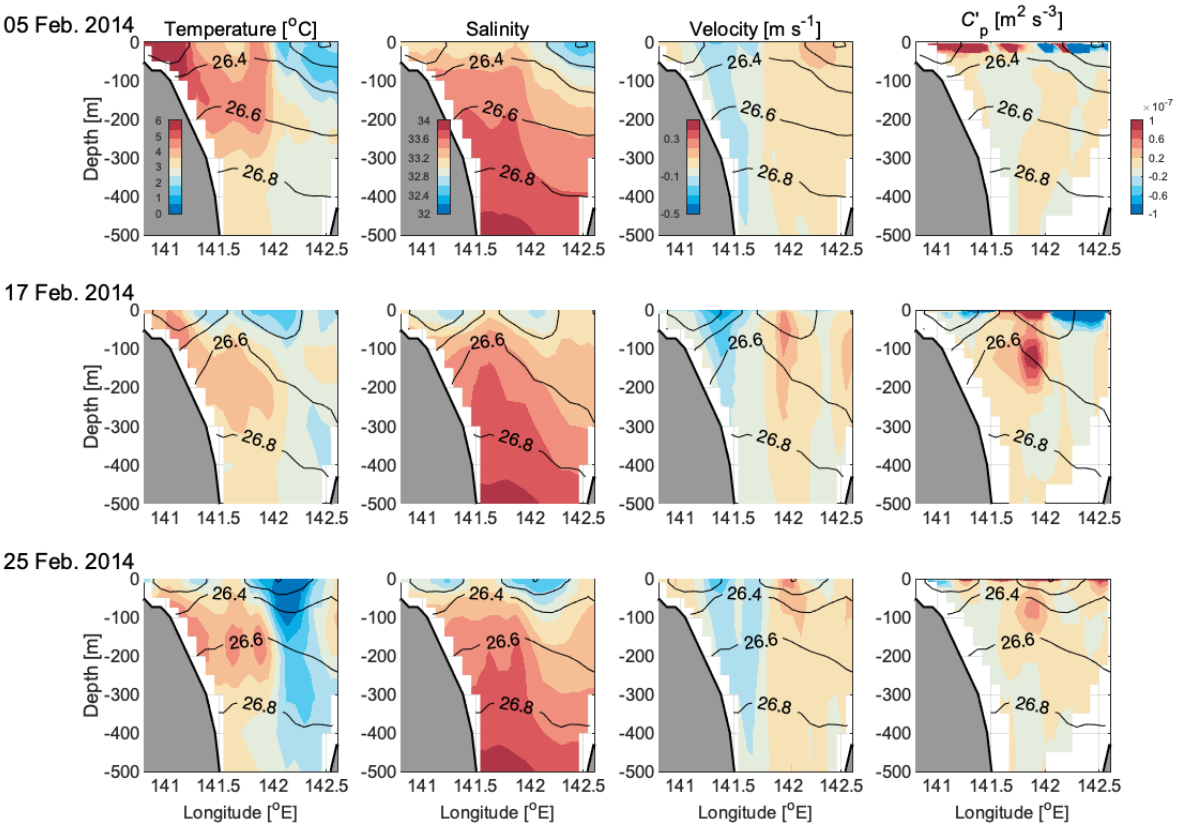

Figure 13. Vertical sections near Funka Bay (at 42.1°N) for February of 2014, estimated from JCOPE2M. From the left, the columns show sections for temperature, salinity, meridional velocity, and energy conversion rate of potential energy C'_{p}, respectively.

4.2 Past cold-water events and variation in the latitude of storm tracks related to the West Pacific pattern

Our results show the importance of atmospheric variations at a timescale of approximately 1 week (such as that associated with migrating lows at mid-latitudes during January to March) to the arrival of COW around Cape Esan. This is a new perspective on the seasonality of the distribution of COW in and around the Tsugaru Strait (including Funka Bay). We suggest that COW might be transported to the west of Cape Erimo more frequently when atmospheric lows pass to the south of mainland Japan during winter. Therefore, the latitude of the storm track may be important to such cold-water events in the eastern Tsugaru Strait with respect to wind direction change, as mentioned above (weakening of

northwesterly monsoon at Cape Erimo), in addition to the effect of wind stress in the Sea of Okhotsk (e.g., Sakamoto et al., 2010; Kuroda et al., 2020).

From the above-mentioned perspective, we examined the association of past cold-water events before 2014 (such as those of 1963, 1974, 1981, 1984, and 2006; Kuroda et al., 2020) with the West Pacific pattern (WP; Wallace and Gutzler, 1981), which is related to the latitude of the storm track (Shimura et al., 2013). Negative anomalies of winter-mean WP show close correspondences with the events of 1963, 1974, 1981, 1984, and 2014 (Fig. 14a). Moreover, the low winter minimum temperatures at Usujiri in 1989 and 1996 correspond closely to the negative WP anomalies. Thus, local atmospheric disturbance through Japan associated with the latitude of the Aleutian Low (which is positively related to the WP; Sugimoto and Hanawa, 2009) should also be an important influence on the distribution of COW. It is noted that the correspondence of the negative WP anomaly with that of salinity from JCOPE2M (Fig. 2d) suggests that not only local atmospheric cooling in and around Hidaka Bay but also transport of low-salinity water from the east would be important to such extreme-cold-water events. In some cases, from 2006 to 2014, the variation in negative WP does not match the low temperature at Usujiri and the salinity estimated by JCOPE2M; however, such cases may be the result of warm water spreading around the outlet region of the Tsugaru Strait to Cape Erimo in association with anticyclonic meso-scale eddies (warm core rings) separated from the Kuroshio Extension (Yasuda et al., 1992; Itoh and Yasuda, 2010a, b; Itoh et al., 2014; Kaneko et al., 2015; Miyama et al., 2021). With regard to the decadal variability in the stability of the Kuroshio Extension (Qiu and Chen, 2005; 2010), 2006–2010 covers a period of the unstable phase (e.g., Kouketsu et al., 2015), and it is expected that numerous pinch-offs of meso-scale eddies from the Kuroshio Extension occurred during this time (e.g., Sugimoto and Hanawa, 2011). Details regarding the effect of meso-scale eddies on the distribution of COW are addressed in the most recent study of our co-authors (Abe et al., in prep.).

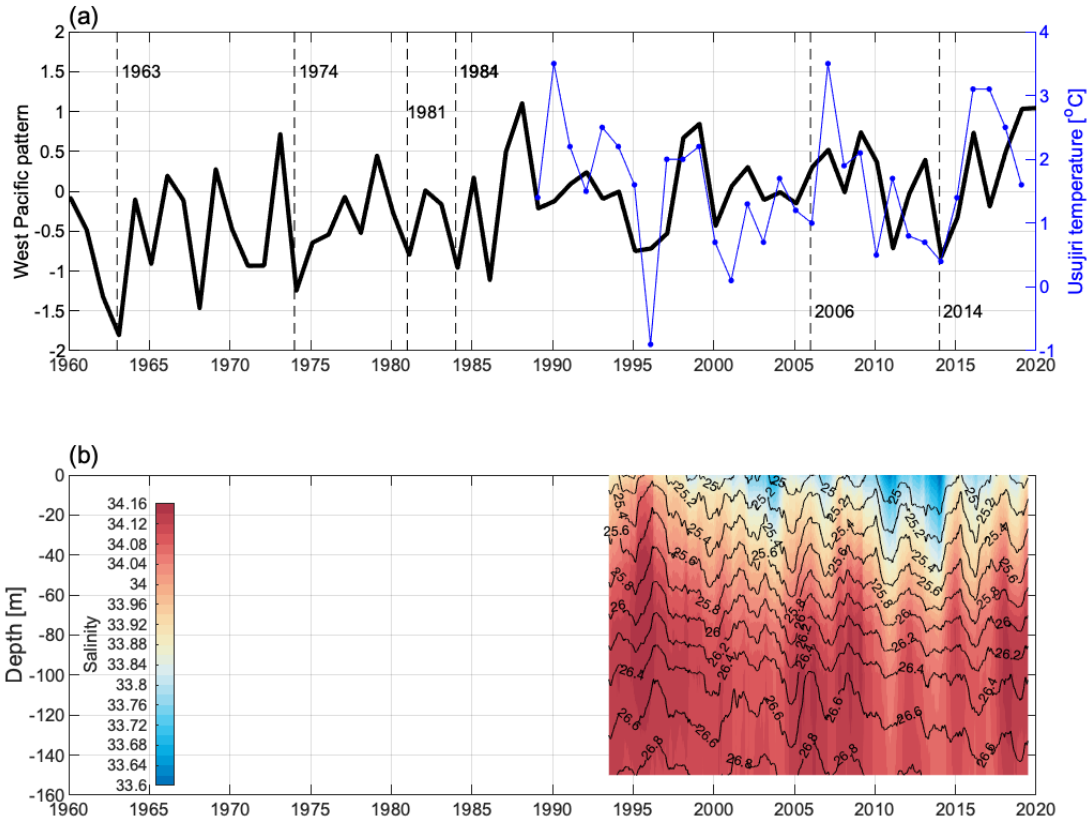

Figure 14. Time series of (**a**) the Western Pacific pattern and surface-water temperature at Usujiri (minimum during January to March for each year), and (**b**) long-term changes in salinity (color) and potential density anomaly (contour; kg m^{-3}) of water within the Tsugaru Strait estimated by JCOPE2M (41.5°N, 140.7°E).

4.3 Long-term change in the inflow water into the Tsugaru Strait from the west

The JOCPE2M outputs show that the density of the inflow water into the strait at depths of <50 m increased over the years following the 2014 event (from = 25.0–25.4 kg m^{-3} to 25.2–25.6 kg m^{-3}; Fig.14b). However, cold-water events similar to that of winter of 2014 in the vicinity of the Shimokita Peninsula have been rare since that time (Figs 2a and 14a). This scarcity of cold-water events is because water on the eastern side of the strait has also become denser in recent years (Fig. 4), on account of the warm and saline water brought by meso-scale eddies, as described above. Abe et al. (in prep.) have reported warmer SSTs for 2017–2019 than 2010–2016 in the region south of Cape Erimo, and they

have defined these periods as cold and warm phases, respectively. During the warm phase, the SST in offshore Hokkaido to Cape Erimo was high, suggesting that the effect of the entry of the cold COW was weak. Thus, the social and economic implications of the cold water appear to have been mitigated. However, acidification may have continued to intensify and extensify in and around the strait, as the inflow of low-pH water from the Sea of Japan is expected to have increased. We also found variations in salinity at depths greater than 50 m of the strait over a 2–4-year timescale from the JCOPE2M output after 1998 (Fig. 14b), implying a possible change in the water-mass type in the western Tsugaru Strait caused by a change in the dominant bifurcations of the Tsushima Warm Current (Fig. 1a) over multiple timescales, such as regime shifts (e.g., 1998/1999) and decadal variations. Therefore, the variation in the inflow of different waters into the strait needs to be monitored continuously using multiple methods, including shipboard observations, an expansion of the HFR system, and routine sampling at the JAMSTEC-MIO, in addition to numerical models.

5 Conclusions

In this study, using data obtained from observations and an ocean data-assimilated model (JCOPE2M), we investigated the extreme-cold-water event in the eastern Tsugaru Strait that occurred during the winter of 2014. Our main findings are as follows.

The studied cold-water intrusion was probably generated at Cape Erimo by a weakening of the northwesterly monsoon owing to a migrating low passing across mainland Japan, which caused low-density COW near the sea surface to enter Hidaka Bay. The low-density, cold COW was transported along the bay as a coastal boundary current to Cape Esan, the northern boundary of the Tsugaru Strait. The COW might also have been affected by the passage of continental shelf waves (topographic Rossby waves) with long wavelength, as well as the effects of baroclinicity, as JCOPE2M outputs suggest a quick barotropic response of the low-salinity anomaly to the wind direction change. The COW partly skipped Funka Bay, which implies the influence of barotropicity. The arrival of the cold water caused an increase in the sea-level difference between the Sea of Japan and the Pacific Ocean, as well as an enhancement of the inflow of the denser JSIW into the strait from the Sea of Japan through nonlinearity of the barotropic continental shelf waves. In the eastern Tsugaru Strait, the difference in density in the horizontal dimension between COW on the northern side of the strait (near Cape Esan) and the JSIW outflow near the southern side (along the northern coast of the Shimokita Peninsula) became large, suggesting that baroclinicity was enhanced through the barotropic process as mentioned above. After the confluence of these two water masses, the horizontal density difference was resolved through dynamical processes, including baroclinic instability, which allowed the extremely cold water to reach the coast of the Shimokita Peninsula. This can be regarded as an example of the response of the Tsugaru Strait system to external disturbance.

With regard to the processes mentioned above, atmospheric disturbance such

as a migrating low is identified as a key driver of such a cold-water event. Past cold-water events (e.g., those in 1974, 1981, 1984, and 1996) show a close correspondence to the timing of negative WP values, suggesting that the southward migration of the storm track is important for such events, in addition to larger-scale wind variation in the Sea of Okhotsk. The risk of such cold-water events occurring near Shimokita Peninsula seems to have become smaller after 2014 because of the more frequent intrusion of high-salinity water masses from the Pacific Ocean into the eastern part of the strait (i.e., the Kuroshio Extension). However, an increase in the near-surface density of the inflowing water to the strait after 2014 is estimated by JCOPE2M. Therefore, the inflow of water into the strait, including the JSIW, should continue to be closely monitored, given the social and economic risks of cold-water events in and around the strait.

Acknowledgments

The authors acknowledge the help of staff of the Mutsu Institute for Oceanography and the Research Institute for Global Change of JAMSTEC. We also sincerely acknowledge the captains and crew of each survey vessel, especially T/S *Ushio-Maru*, for their warm cooperation during sample collection and hydrographic measurements during cruises. We thank Dr. H. Munehara for providing temperature data at Usujiri. We also acknowledge the technical support staff from Marine Work Japan. We are grateful to the editor and anonymous reviewers for their valuable and insightful comments on an earlier version of this paper.

Open research

The data for HFR, temperature, and the HO-line used in the present study are distributed through JAMSTEC-MIO (https://www.godac.jamstec.go.jp/morset s/e/top/). The output of JCOPE2M is distributed from Application Laboratory, JAMSTEC (https://www.jamstec.go.jp/apl/e/). Wind speed data are available from the Japan Oceanographic Data Center (https://jdoss1.jodc.go.jp/vpage/ wave.html). Data for the A-line (KS1308) are distributed from the following site: https://ocean.fra.go.jp/a-line/a-line_index.html (http://www.data.jma .go.jp/gmd/kaiyou/shindan/index_obs.html). Values of the WP index are provided by the National Weather Service, National Oceanic and Atmospheric Administration (https://www.cpc.ncep.noaa.gov/data/teledoc/wp.shtml).

References

Astor, Y. M., Lorenzoni, L., Thunell, R., Varela, R., Muller-Karger, F., Troccoli, L., et al. (2013). Interannual variability in sea surface temperature and fCO2 changes in the Cariaco Basin. *Deep Sea Research Part II: Topical Studies in Oceanography*, 93, 33–43. https://doi. org/10.1016/j.dsr2.2013.01.002

Brooks, I. H., Niiler, P. P. (1977). Energetics of Florida current. *Journal of Marine Research*, *35*, 163–191.

Csanady, G. T. (1985). ‘‘Pycnobatic’’ currents over the upper continental slope. *Journal of Physical Oceanography*, *15*, 306–315.

Dewar, W. K., Bane, J. M. (1989). Gulf-stream dynamics. part II: Eddy energetics at 73°W. *Journal of Physical Oceanography. 19,* 1574–1587. https://doi.org/10.1175/1520-0485(1989)019%3c1574:GSDPIE%3e2.0.CO;2

Dore, J. E., Lukas, R., Sadler, D. W., Church, M. J., & Karl, D. M. (2009). Physical and biogeochemical modulation of ocean acidification in the central North Pacific. *Proceedings of the National Academy of Sciences of the United States of America*, *106*, 12235–12240. https:// doi.org/10.1073/pnas.0906044106

Gill, A. E. (1976). Adjustment under gravity in a rotating channel, *Journal of Fluid Mechanics*, 77, 603-621. https://doi.org/10.1017/S0022112076002280

Gill, A. E. (1982). Atmosphere-ocean dynamics (p. 662). Academic Press.

Gill, A. E. and Schumann, E. H. (1974). The generation of long shelf waves by the wind. *Journal of Physical Oceanography,4*,83–90. https://doi.org/10.1175/1520-0485(1974)004<0083:TGOLSW>2.0.CO;2

Hanawa, K., & Mitsudera, H. (1987). Variation of water system distribution in the Sanriku coastal area. *Journal of the Oceanographical Society of Japan*, *42*, 435-446. https://doi.org/10.1007/BF02110194

Higaki, N., Isoda, Y., Isogai, Y., & Yahaba., H. (2008). Seasonal Variations of Water System Distributions and Flow Patterns off the West Coast of Hokkaido. *Oceanography in Japan*, *17*(4), 223–240. (in Japanese with English abstract).

Huthnance, J. M. (1984). Slope currents and “JEBAR”. *Journal of Physical Oceanography*, *14*, 795–810. https://doi.org/10.1175/1520-0485(1984)014<0795:SCA>2.0.CO;2

Ida, S., Yamashita, S., Isoda, Y., & Kobayashi, N. (2016). Inflow process of low potential vorticity water originating from the intermediate waters of the Japan Sea into the Tsugaru Strait, *Oceanography in Japan*, *25*(4), 101–122. (in Japanese with English abstract).

Igeta, Y., Yankovsky, A., Fukudome, K., Ikeda, S., Okei, N., Ayukawa, K., Kaneda, A., Watanabe, T. (2017). Transition of the Tsushima Warm Current Path Observed over Toyama Trough, Japan. *Journal of Physical Oceanography*, 21 47 (11), 2721–2739. https://doi.org/10.1175/jpo-d-17-0027.1

Isobe, A. (1994). Seasonal variation of the vertically averaged flow caused by the Jebar effect in the Tsushima Strait. *Journal of Oceanography*, *50*, 617–633.

Isobe, A., & Isoda, Y. (1997). Circulation in the Japan Basin, the northern part of the Japan Sea. *Journal of Oceanography*, *53*, 373–381.

Itoh, S., & Sugimoto, T. (2008). Current variability of the Kuroshio near the separation point from the western boundary. *Journal of Geophysical Research*,

113, C11020, doi:10.1029/2007JC004682

Itoh, S., & Yasuda, I. (2010a). Characteristics of mesoscale eddies in the Kuroshio-Oyashio extension region detected from the distribution of the sea surface height anomaly. *Journal of Physical Oceanography*, 40, 1018–1034. doi:10.1175/2009JPO4265.1.

Itoh, S., & Yasuda, I. (2010b). Water mass structure of warm and cold anticyclonic eddies in the western boundary region of the Subarctic North Pacific. *Journal of Physical Oceanography*, *40*, 2624–2642. doi:10.1175/2010JPO4475.1.

Itoh, S., Yasuda, I., Ueno, H., Suga, T., & Kakehi, S. (2014). Regeneration of a warm anticyclonic ring by cold water masses within the western subarctic gyre of the North Pacific, *Journal of Oceanography*, *70*(3), 211–223. doi:10.1007/s10872-014-0225-9.

Kaneko, H., Itoh, S., Kouketsu, S., Okunishi, T., Hosoda, S., & Suga, T. (2015). Evolution and modulation of a poleward-propagating anticyclonic eddy along the Japan and Kuril-Kamchatka trenches. *Journal of Geophysical Research: Oceans*, *120*(6), 4418–4440. doi:10.1002/2014JC010693.

Kaneko, H., Sasaki, K., Abe, H., Tanaka, T., Wakita, M., Watanabe, S., Okunishi, T., Sato, Y., & Tatamisashi, S. (2021). The Role of an Intense Jet in the Tsugaru Strait in the Formation of the Outflow Gyre Revealed Using High-Frequency Radar Data, *Geophysical Researsh Letters*, https://doi.org/10.1029/2021GL092909

Kobayashi, N. Isoda, Y., Kobayashi, M., Satoh, C., Kimura, O., Yamagushi, H., Takatsu T., & Rosa, A. L. (2009). The *Kyucho* occurred off Kameda Peninsula, Hokkaido, at the end of May, 2006. *Bulletin of Fisheries Sciences, Hokkaido University*, *58*(3), 29–41. (in Japanese with English abstract).

Kono, T., Foreman, M., Chandler, P., & Kashiwai, M. (2004). Coastal Oyashio south of Hokkaido, Japan. *Journal of Physical Oceanography*, *34*, 1477–1494. https://doi.org/10.1175/1520-0485(2004)034%3c1477:COSOHJ%3e2.0.CO;2

Kouketsu, S., Kaneko, H., Okunishi, T., Sasaoka, K., Itoh, S., Inoue, R., Ueno, H. (2015). Mesoscale eddy effects on temporal variability of surface chlorophyll a in the Kuroshio Extension. *Journal of Oceanography*, *72*(3), 439–451. DOI 10.1007/s10872-015-0286-4

Kubokawa, A. & Hanawa, K. (1984). A Theory of Semigeostrophic Gravity Waves and its Application to the Intrusion of a Density Current along a Coast. Part 2. Intrusion of a Density Current along a Coast in a Rotating Fluid. *Journal of Oceanography Society of Japan.* *40*(4), 260–270. https://doi.org/10.1007/BF02302519

Kuroda, H., Kubo, M., Isoda, Y., Takeoka, H., & Honda, S. (2005). Subtidal current variations on the eastern shelf of Hidaka Bay. *Bulletin of Fisheries Sciences, Hokkaido University*, *56*(2), 43–53. (in Japanese with English abstract).

Kuroda, H., Isoda, Y., Takeoka, H., Kuma, K., Honda, S., Matsuura, H., et al. (2012). Intrusion of the Oyashio water into the eastern mouth of Tsugaru Strait in early summer, 2003. *Continental Shelf Research*, *32*, 36–46. https://doi.org/10.1016/j.csr.2011.10.012

Kuroda, H., Toya, Y., Kakehi, S., & Setou, T. (2020). Interdecadal variations of the Oyashio and extreme cold water events near the Japanese coast from the 1960s to the 2010s, in Changing Asia-Pacific Marginal Seas, eds C.-T. A. Chen and X. Guo (Singapore: Springer), 217–244. doi: 10.1007/978-981-15-4886-4_13

Mellor, G. L., Hakkinen, S., Ezer, T., & Patchen, R. (2002). A generalization of a sigma coordinate ocean model and an inter comparison of model vertical grids. In: Pinardi N, Woods JD (eds) Ocean Forecasting: Conceptual Basis and Applications. Springer, New York, pp 55–72

Mertz, G., & Wright, D. G. (1992). Interpretations of the JEBAR term. *Journal of Physical Oceanography*, *22*, 301–305. https://doi.org/10.1175/1520-0485(1992)022%3c0301:IOTJT%3e2.0.CO;2

Miyama, T., Minobe, S., & Goto, H. (2021). Marine heatwave of sea surface temperature of the Oyashio region in summer in 2010–2016. *Marine fisheries, Aquaculture and Living Resources*, 7:576240. https://doi.org/10.3389/fmars.2020.576240

Miyazawa, Y., Zhang, R. C., Guo, X., Tamura, H., Ambe, D., Lee, J. S., Okuno, A., Yoshinari, H., Setou, T., Komatsu, K. (2009). Water mass variability in the Western North Pacific detected in a 15-year eddy resolving ocean reanalysis. *Journal of Oceanography*, *65*, 737–756.

Miyazawa, Y., Varlamov, S. M., Miyama, T. Guo, X., Hihara, T., Kiyomatsu, K., Kachi, M., Kurihara, Y., & Murakami, H. (2017). Assimilation of high-resolution sea surface temperature data into an operational nowcast/forecast system around Japan using a multi-scale three-dimensional variational scheme. *Ocean Dynamics*. *67*, 713–728. DOI 10.1007/s10236-017-1056-1

Miyazawa, Y., Varlamov, S. M., Miyama, T., Kurihara, Y., Murakami, H., & Kachi, M. (2021). A Nowcast/Forecast System for Japan's Coasts Using Daily Assimilation of Remote Sensing and In Situ Data. *Remote Sensing*. https://doi.org/10.3390/ rs13132431

Murakami, T. (1984). "Inflow of the Coastal Oyashio into the southern area of the Hokkaido Island. ". *Marine sciences monthly*, *16*(12), 697–701 (in Japanese).

Nakamura, T., Awaji, T., Toyoda, T., & Ishikawa, Y. (2003). Coastal Oyashio in a North Pacific simulation experiment. *Bulletin on Coastal Oceanography*, *41*, 13–22 (in Japanese with English abstract).

Nishida, Y., Kanomata, I., Tanaka, I., Sato, S., Shingo, T., & Matsubara, H. (2003). Seasonal and interannual variations of the volume transport through

the Tsugaru Strait. *Oceanography in Japan*, *12*(5), 487–499. https://doi.org/10.5928/kaiyou.12.487. (in Japanese with English abstract)

Ohshima, K., & Miyake, H. (1990). A numerical Study of Wind-Induced Circulation off Southern Coast of Hokkaido and in Funka Bay. *Sea and Sky*, *66*, 2, 53–66. (in Japanese with English abstract).

Ohshima, K. (1994). The flow system in the Japan Sea caused by a sea level difference through shallow straits. *Journal of Geophysical Research*, *99*, C5, 9925–9940. https://doi.org/10.1029/94JC00170.

Qiu, B., & Chen, S. (2005). Eddy-induced heat transport in the subtropical North Pacific from Argo, TMI, and altimetry measurements. *Journal of Physical Oceanography*, *35*, 458–473. doi:10.1175/JPO2696.1.

Qiu, B., & Chen, S. (2010). Eddy-mean flow interaction in the decadally modulating Kuroshio Extension system. *Deep Sea Research Part II*, *57*, 13–14, 1098–1110. https://doi.org/10.1016/j.dsr2.2008.11.036

Rosa, A. L., Isoda, Y., Uehara, K., & Aiki, T. (2007). Seasonal variations of water system distribution and flow patterns in the Southern Sea Area of Hokkaido, Japan. *Journal of Oceanography*, *63*, 573–588. https://doi.org/10.1007/s10872-007-0051-4

Sakamoto, K., Tsujino, H., Nishikawa, S., Nakano, H., & Motoi, T. (2010). Dynamics of the Coastal Oyashio and its seasonal variation in a high-resolution western North Pacific Ocean model. *Journal of Physical Oceanography*, *40*(6), 1283–1301. https://doi.org/10.1175/2010JPO4307.1

Senjyu, T. (1999). The Japan Sea Intermediate Water; Its Characteristics and Circulation. *Journal of Oceanography*, *55*, 111–122.

Shaw, P., & Csanady, G. T. (1983). Self-advection of density perturbations on a sloping continental shelf. *Journal of Physical Oceanography*, *13*, 769–782. https://doi.org/10.1175/1520-0485(1983)013%3c0769:SAODPO%3e2.0.CO;2

Shimura, T., Mori, N., & Mase, H. (2013). Ocean Waves and Teleconnection Patterns in the Northern Hemisphere. *Journal of Climate*, *26*(1), 8654–8670. https://doi.org/10.1175/JCLI-D-12-00397.1

Sugimoto, S., & Hanawa, K. (2009). Decadal and Interdecadal Variations of the Aleutian Low Activity and Their Relation to Upper Oceanic Variations over the North Pacific. *Journal of the Meteorological Society of Japan*, *87*(4), 601–614. DOI:10.2151/jmsj.87.601

Sugimoto, S., & Hanawa, K. (2011). Roles of SST anomalies on the wintertime turbulent heat fluxes in the Kuroshio-Oyashio Confluence Region: Influences of warm eddies detached from the Kuroshio Extension. *Journal of Climate*, *24*(24), 6551–6561. https://doi.org/10.1175/2011JCLI4023.1

Tanaka, I. (1984). Distribution of Chlorophyll *a* at the Frontal Region Formed in the Waters Adjacent to Funka Bay, Hokkaido. *Bulletin of the Japanese Society*

of Fisheries Oceanography, *46*, 9–17. (in Japanese with English abstract).

Wagawa, T., Kawaguchi, Y. Igeta, Y. Honda, N., Okunishi T., & Yabe, I. (2020) Observations of oceanic fronts and water-mass properties in the central Japan Sea: Repeated surveys from an underwater glider. *Journal of Marine Systems*, *201*, 103242, https://doi.org/10.1016/j.jmarsys.2019.103242

Wakita, M., Nagano, A., Fujiki, T., & Watanabe, S. (2017). Slow acidification of the winter mixed layer in the subarctic western North Pacific. *Journal of Geophysical Research: Oceans*, *122*, 6923–6935. https://doi.org/10.1002/2017JC013002

Wakita, M., Sasaki, K., Nagano, A., Abe, H., Tanaka T., Nagano, K, et al. (2021). Rapid reduction of pH and CaCO3 saturation state in the Tsugaru Strait by the intensified Tsugaru Warm Current during 2012-2019. *Geophysical Research Letters*, *48*. https://doi.org/10.1029/2020GL091332

Wallace, J., M., & Gutzler, D. S. (1981). Teleconnections in the Geopotential Height Field during the Northern Hemisphere Winter. *Monthly Weather Review*, *109*, 784–812. http://dx.doi.org/10.1175/1520-0493(1981)109%3c0784:TITGHF%3e2.0.CO;2

Yamagata, T. (1980). A Theory for Propagation of an Oceanic Warm Front with Application to Sagami Bay. Tellus, *32*(1), 73–76. https://doi.org/10.3402/tellusa.v32i2.10482

Yasuda, I., Okuda, K., & Hirai, M. (1992). Evolution of a Kuroshio Warm-Core Ring - Variability of the Hydrographic Structure, *Deep-Sea Research*, *39*(1A), S131–S161. https://doi.org/10.1016/S0198-0149(11)80009-9

Yasuda, I., Okuda, K., & Shimizu, Y. (1996). Distribution and modification of north Pacific intermediate water in the Kuroshio-Oyashio interfrontal zone, *Journal of Physsical Oceanography*, *26*, 448–465. doi:10.1175/1520-0485(1996)026<0448:DAMONP>2.0.CO;2

Yasui T, Abe H, Hirawake T, Sasaki K, Wakita M (accepted). Seasonal pathways of the Tsugaru Warm Current revealed by high-frequency ocean radars, *Journal of Oceanography*.

References for the Supporting Information

Japan Meteorological Agency/Japan. 2013, updated monthly. JRA-55: Japanese 55-year Reanalysis, Daily 3-Hourly and 6-Hourly Data. Research Data Archive at the National Center for Atmospheric Research, Computational and Information Systems Laboratory. https://doi.org/10.5065/D6HH6H41. Accessed on 17 February 2022.